mathematics

MDPI

Article

On the throughput of the common target area for robotic swarm strategies

Yuri Tavares dos Passos [1,2]*, Xavier Duquesne [2] and Leandro Soriano Marcolino [2]

[1] Centro de Ciências Exatas e Tecnológicas, Universidade Federal do Reconcâvo da Bahia, Rua Rui Barbosa, 710. Centro., Cruz das Almas, 44380-000, Brazil
[2] School of Computing and Communications, Lancaster University, Bailrigg, Lancaster LA1 4WA, UK; duquesne.xavier.13@gmail.com (X.D.); l.marcolino@lancaster.ac.uk (L.S.M.)
* Correspondence: yuri.passos@ufrb.edu.br

check for updates

Citation: Passos, Y.T.; Duquesne, X.; Marcolino, L.S. On the throughput of the common target area for robotic swarm strategies. *Mathematics* **2022**, *10*, 2482. https://doi.org/10.3390/math10142482

Academic Editors: Jiangping Hu and Zhinan Peng
Received: 12 June 2022
Accepted: 14 July 2022
Published:

Proof of Lemma 1

Let $l_\theta(t) = \sqrt{(x_1(t) - x_2(t))^2 + (y_1(t) - y_2(t))^2}$ be the distance between the two robots. The robots must maintain their minimum distance d at all time:

$$\forall t \in \mathbb{R}, l_\theta(t) \geq d. \tag{S1}$$

To avoid a collision, $\theta \neq \pi$, which corresponds to the case where robots face each other exactly. As a result, $\cos(\theta) \neq -1$. For ease of calculation, define $X = \tau v$, that is, the distance between Robot 1 and Robot 2 when Robot 1 reaches the target. Also define $P_\theta(t) = l_\theta(t)^2 - d^2$, so the constraint in (S1) for the distance between them is expressed by $\forall t \in \mathbb{R}, l_\theta(t) \geq d \Leftrightarrow \forall t \in \mathbb{R}, P_\theta(t) \geq 0$. In addition, $P_\theta(t) = 2(1 - \cos(\theta))v^2t^2 - 2X(1 - \cos(\theta))vt + X^2 - d^2$, where $\cos(\theta) = \cos(\theta_2 - \theta_1) = \cos(\theta_2)\cos(\theta_1) + \sin(\theta_2)\sin(\theta_1)$ is used.

Two cases are identified:

1. Case 1: $\cos(\theta) \neq 1$. Then $P_\theta(t)$ is a second-degree polynomial in t. It is of the form $at^2 + bt + c$ with $a = 2(1 - \cos(\theta))v^2$, $b = -2X(1 - \cos(\theta))v$ and $c = X^2 - d^2$. $P_\theta(t)$ has a with positive sign for all t, because $(1 - \cos(\theta)) > 0$ when $\cos(\theta) \neq 1$. Thus, as $a > 0$, by second-degree polynomial inequalities properties, $P_\theta(t) \geq 0$ for all t if and only if its discriminant $\Delta = b^2 - 4ac$ is negative, that is, $\forall t \in \mathbb{R}, P_\theta(t) \geq 0 \Leftrightarrow b^2 - 4ac \leq 0$. Thus,

$$X \geq d\sqrt{\frac{2}{1 + \cos(\theta)}} \tag{S2}$$

2. Case 2: $\cos(\theta) = 1$. Then $P_\theta(t) = X^2 - d^2$. In this case, $P_\theta(t) \geq 0$ for all t when $X^2 - d^2 \geq 0 \Rightarrow X \geq d$. This is the same as using $\cos(\theta) = 1$ in (S2).

Hence, (S2) gives, for the robots to respect the minimum distance d for every time t, a relation between the minimum distance, the angle between the lanes and the distance between Robot 1 and Robot 2 when Robot 1 reaches the target. The final result is obtained by noticing that (S2) is equivalent to $\tau \geq \frac{d}{v}\sqrt{\frac{2}{1+\cos(\theta)}}$.

Proof of Proposition 1

It is shown by induction on N, which is the number of robots moving towards the target. Define θ_N as the angle between the trajectories of Robot $N-1$ and Robot N; τ_N, the minimum delay between the arrival of Robot $N-1$ and Robot N; and Δ_N, the minimum delay between the arrival of Robot 1 and Robot N. The aim is to show the following predicate: for all $N \geq 2$, $\Delta_N = (N-1)d/v$ for $\theta_2 = \theta_3 = \ldots = \theta_N = 0$.

Base case ($N = 2$): Let τ_2 be the delay between the arrival of Robot 1 and Robot 2. From Lemma 1, the minimum delay between Robot 1 and Robot 2 is equal to $\frac{d}{v}\sqrt{\frac{2}{1+\cos(\theta_2)}}$,

which is minimised by $\theta_2 = 0$. Then, the minimum delay between the two robots is $\tau_2 = d/v = \Delta_2$.

Inductive step: suppose the predicate is true for a given $N-1 \geq 2$. It will be shown that this implies the predicate is true for N robots. As in the previous case, it is concluded from Lemma 1 that the minimum delay between Robot $N-1$ and Robot N is equal to $\frac{d}{v}\sqrt{\frac{2}{1+\cos(\theta_N)}}$, which is minimised by $\theta_N = 0$. Then, the minimum delay between the two robots is $\tau_N = d/v$, thus

$\Delta_N = \Delta_{N-1} + \tau_N = (N-2)\frac{d}{v} + \frac{d}{v} = (N-1)\frac{d}{v}$. Consequently, the minimum delay between Robot 1 and Robot N is $\Delta_N = \sum_{i=2}^{N} \tau_i = (N-1)\frac{d}{v}$ and the time of arrival of Robot N, for all N, is minimised by $\theta_2 = \theta_3 = \ldots = \theta_N = 0$. Finally, by Definition 2, the throughput is $f = \frac{N-1}{\Delta_N} = \frac{v}{d}$.

Proof of Proposition 2

Consider Figure 3. The distance between the lanes is $2s$, and the distance between two robots is d. Thus, $d_p = \sqrt{d^2 - (2s)^2}$. Hence, the distance between two robots in the same lane is $d_e = 2d_p = 2\sqrt{d^2 - (2s)^2}$.

The distance between two robots in the same lane must not be less than d, so $d_e \geq d$. This is true, because, as $0 < s \leq \frac{\sqrt{3}}{4}d$, $d_e = 2\sqrt{d^2 - (2s)^2} \geq 2\sqrt{d^2 - \left(2\frac{\sqrt{3}}{4}d\right)^2} = d$.

Without loss of generality, assume the first robot to reach the target area being at the top lane in Figure 3. The number of robots on any lane is the integer division of the size of the lane by the offset between the robots plus one (because the first robot is included in this counting). Therefore, the number of robots for a given time T in the top lane is $N_1(T) = \left\lfloor \frac{vT}{d_e} + 1 \right\rfloor$ and in the bottom lane is $N_2(T) = \left\lfloor \frac{vT - d_p}{d_e} + 1 \right\rfloor = \left\lfloor \frac{vT}{d_e} + \frac{1}{2} \right\rfloor$. By Definition 2, $f(T) = \frac{N_1(T)+N_2(T)-1}{T} = \frac{1}{T}\left(\left\lfloor \frac{vT}{2\sqrt{d^2-(2s)^2}} \right\rfloor + \left\lfloor \frac{vT}{2\sqrt{d^2-(2s)^2}} + \frac{1}{2} \right\rfloor \right)$. By the definition of the floor function, $\lfloor x \rfloor = x - frac(x)$ with $0 \leq frac(x) < 1$. Thus, $\lim_{T\to\infty} f(T) = \frac{v}{d\sqrt{1-(2s/d)^2}}$, as $\lim_{T\to\infty} \frac{frac(x)}{T} = 0$, for any x.

Proof of Proposition 3

As the distance between the robots must be at least d and $\frac{\sqrt{3}}{4}d < s < \frac{d}{2}$, $d_p = d/2$ is assigned in Figure 3. By doing so, two robots side by side in one lane and a robot in the other lane form an equilateral triangle with a side measuring d, whose height has size $\frac{\sqrt{3}}{2}d$. Hence, the minimum diameter of the circular target region must be this value, and the hypothesis says so.

Moreover, the radius of the target area is less than $d/2$, implying that the three robots in Figure 3 must stay in the equilateral triangle formation because the two lanes cannot be far by d units of distance.

Thus, the throughput for a given time T is calculated similarly as in Proposition 2, resulting $f(T) = \frac{1}{T}\left(\left\lfloor \frac{vT}{d} \right\rfloor + \left\lfloor \frac{vT}{d} + \frac{1}{2} \right\rfloor \right)$ and $f = \lim_{T\to\infty} f(T) = \frac{2v}{d}$.

Proof of Proposition 4

When robots move in straight lines in a single lane, the optimal throughput is $\frac{v}{d}$ (Proposition 1). Since $s \geq \frac{d}{2}$, multiple straight line lanes can be parallel to each other (Figure 4).

As the robots are going to a circular target region, the robots next to the centre reach the region in a shorter time than the others. The first robot of each lane must run an additional distance d_i from the beginning of its lane, which is related to its y-coordinate. Figure S1 illustrates this distance for a robot in Lane i. The right triangle ABC has hypotenuse $\overline{AC}$ measuring s, so the horizontal cathetus $\overline{AB}$ measures $\sqrt{s^2 - (s-(i-1)d)^2}$. Consequently,

the robot in the Lane i needs to walk an additional distance represented by $\overline{BD}$, which has $d_i = |\overline{BD}| = s - |\overline{AB}| = s - \sqrt{s^2 - (s-(i-1)d)^2}$ units of length.

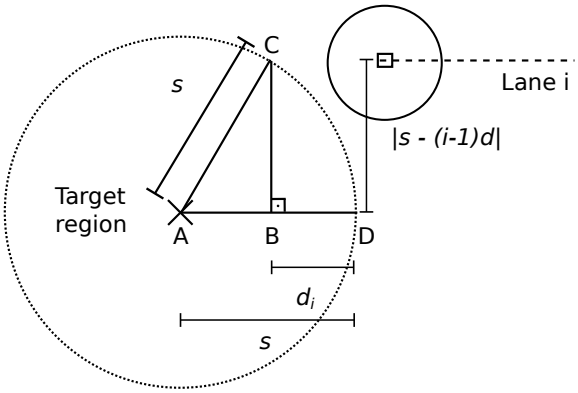

Figure S1. The distance from the target region to a robot at the beginning of the Lane i is equal to d_i (represented by $\overline{BD}$).

This distance is minimised when $|\overline{BD}| = 0$, that would happen if $i = \frac{s}{d} + 1$. However, i must be integer, so $|\overline{BD}|$ is minimised by an integer J that minimises d_J. If $\frac{s}{d} \notin \mathbb{Z}$, the two nearest integers are $\lfloor \frac{s}{d} \rfloor$ and $\lceil \frac{s}{d} \rceil$. Thus, if $J = \lfloor \frac{s}{d} \rfloor + 1$ then, equivalently, $d_{\lfloor \frac{s}{d} \rfloor + 1} \leq d_{\lceil \frac{s}{d} \rceil + 1} \Leftrightarrow \left| s - \lfloor \frac{s}{d} \rfloor d \right| \leq \left| s - \lceil \frac{s}{d} \rceil d \right|$. Thus, $J = \lfloor \frac{s}{d} \rfloor + 1$, if $\left| s - \lfloor \frac{s}{d} \rfloor d \right| \leq \left| s - \lceil \frac{s}{d} \rceil d \right|$, otherwise, $J = \lceil \frac{s}{d} \rceil + 1$.

Let $N(T)$ be the number of robots that arrive at the target region until a given time T after the first robot has reached it. Thus, $N(T) = \sum_{i=1}^{\lfloor \frac{2s}{d} \rfloor + 1} N_i(T)$, where $N_i(T)$ is the number of robots at Lane i that arrived at the target region by time T. As every robot has the same linear speed and started at the same x-coordinate, when the first robot at Lane J reaches the target region, all robots have run d_J units of length. Hence, at each Lane i, instead of running an additional d_i to reach the target region, they need to run $d_i - d_J$. Consequently, $N_i(T) = \left\lfloor \frac{vT - (d_i - d_J)}{d} + 1 \right\rfloor$, if $T \geq \frac{d_i - d_J}{v}$, otherwise, $N_i(T) = 0$, and, by Definition 2, $f_p(T) = \frac{N(T)-1}{T} = \frac{1}{T}\left(\sum_{i=1}^{\lfloor \frac{2s}{d} \rfloor + 1} N_i(T) \right) - \frac{1}{T}$. Also, $f_p = \lim_{T \to \infty} f_p(T) = \left\lfloor \frac{2s}{d} + 1 \right\rfloor \frac{v}{d}$, as $frac$ and d_i are bounded for every i due to $0 \leq d_i \leq s$ and $0 \leq frac(x) < 1$ for any x.

Proof of Proposition 5

Without loss of generality, consider the target at the origin of a coordinate system and that the robots are moving parallel to the x-axis. By Definition 2, the throughput considers the number of robots that cross the target during a unit of time and after the first robot has reached it. The number of robots, N_T, is evaluated during a time T. As a result, computing the maximum throughput is reduced to finding the maximum number of robots (their centre of mass) that can fit in a rectangle of width $w(T) = vT$ and height $h = 2s$.

Figure S2 illustrates how N_T is calculated. Robots are represented by black dots in hexagonal formation and distant by d. In (I), only the first robot reached the target. In (II), all robots not in the dashed area arrived in the target region before the last robot. The robots on the right dashed area should not be counted because their arrival time is greater than the arrival time of the last robot. Hence, they arrive after the considered time frame T. That is, all robots on the dashed area in (I) should be counted as part of the number of robots that reached the target region in the time between the first and the last robot, while the robots on the dashed area in (II) should not. As these dashed areas have the same value, this proof considers the number of robots inside a rectangle $vT \times 2s$. Then, the dashed area used for counting in (II) replaces the unconsidered robots in the dashed area in (I). As $T \to \infty$ is of concern, any possible difference between the number of robots on the dashed areas of either side due to the configuration of the hexagonal packing is negligible.

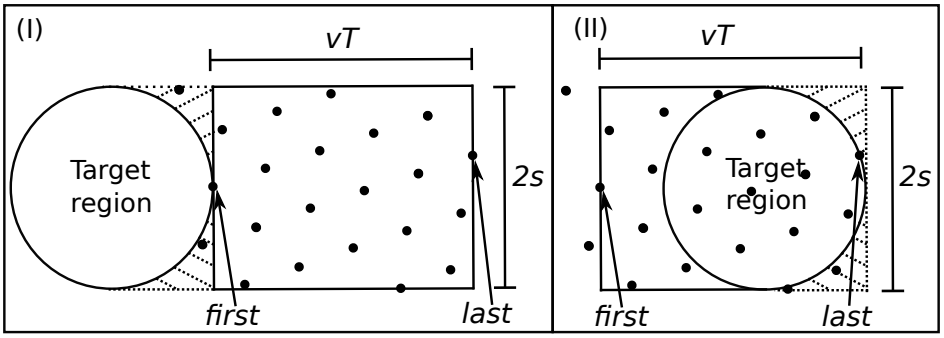

Figure S2. The rectangular area regarding the calculation of N_T over time.

Due to the constraint that robots must be at a distance d from each other, consider discs of radius $d/2$ as reserved areas for each robot, and any two reserved areas must not intersect. Therefore, the problem is equivalent to finding the optimal arrangement of circles of radius $d/2$ in a rectangle of width $W(T) = w(T) + 2\frac{d}{2}$ and height $H = h + 2\frac{d}{2}$. This formulation is a variant of the *circle packing* problem, which is already well studied. (See http://packomania.com/ and http://hydra.nat.uni-magdeburg.de/packing/crc_var/crc.html, acessed on 16 November 2021, for an informal introduction.) The term $2\frac{d}{2}$ was added because the circle packing problem deals with full circles, not their centres.

The optimal surface occupied by the circles divided by the rectangle area was proven to be $\pi\sqrt{3}/6$ in the case of hexagonal packing over an infinite area [1]. Thus, the total area occupied by the circles representing the reserved areas of the robots is given by $\left(\pi\sqrt{3}/6\right)HW(T)$. Hence, the maximum number of robots N_T that can fit inside the $HW(T)$ area is bounded by $N_{opt}(T) \geq N_T$, for $N_{opt}(T) = \left\lfloor \frac{\left(\pi\sqrt{3}/6\right)HW(T)}{\pi d^2/4} \right\rfloor = \left\lfloor \frac{2HW(T)}{\sqrt{3}d^2} \right\rfloor$. By Definition 2, the maximum throughput is $f_h^{max}(T) = \frac{N_{opt}(T)-1}{T} = \frac{\left\lfloor \frac{2HW(T)}{\sqrt{3}d^2} \right\rfloor - 1}{T}$. As for any x, $\lfloor x \rfloor = x - frac(x)$ and $0 \leq frac(x) < 1$, the upper bound of the asymptotic throughput is $f_h^{max} = \lim_{T\to\infty} f_h^{max}(T) = \frac{2}{\sqrt{3}}\left(\frac{2s}{d} + 1\right)\frac{v}{d}$.

Proof of Proposition 6

This proof concerns about the throughput of the target region for a given time and hexagonal packing angle θ, $f_h(T,\theta) = \frac{N(T,\theta)-1}{T}$, where $N(T,\theta)$ denotes the number of robots which arrived at the target region. Figure S3 illustrates the arrival of the robots on the target region.

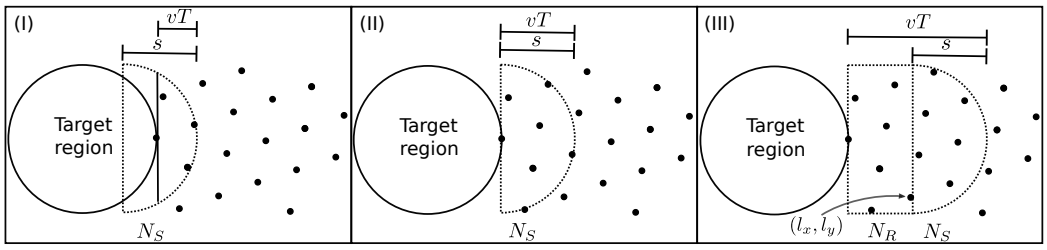

Figure S3. Arrival of the robots on the target region over time.

In Figure S3 (I), when the robots – here represented by black dots – in hexagonal packing begin to arrive at the target region, only the robots inside a part of the semicircle are counted. In Figure S3 (II), consider the first robot to reach the target region being at (x_0, y_0) at time 0. As T grows, this continues until $vT = s$. In Figure S3 (III), when $vT > s$, the robots are counted on two regions: a rectangular, N_R, and a semicircular, N_S. When $vT > s$, the semicircular region counting starts after the last robot on the rectangular region located at (l_x, l_y).

As this region has a circular shape, not all robots at the distance vT arrive at target region by the time T. Thence, the number of robots in hexagonal packing are divided into the number of robots located inside a rectangle, N_R, and of robots inside a semicircle N_S (Figure S3 (III)). That is, $N(T,\theta) = N_S(T,\theta) + N_R(T,\theta)$ and $N_R = 0$ whenever $vT \leq s$.

This proof is divided in lemmas for helping the construction of the equation to compute $N_R(T,\theta)$ and $N_S(T,\theta)$ as well for calculating $\lim_{T\to\infty} f_h(T,\theta)$. Before presenting them, it is discussed a coordinate space transformation which will be used to count the robots for N_R and N_S. This transformation was inspired by [2].

Figure S4 shows the coordinate spaces used in this proof: the usual Euclidean space (x,y) in relation to the target region and the rectangle region formed by robots in hexagonal packing going to it; the coordinate space (x_g,y_g), formed by the usual space after a translation to the first robot to reach the target region at (x_0,y_0), followed by a rotation by $-\psi$; the coordinate space (x_h,y_h), a hexagonal grid coordinate space made after this transformation and a linear transformation H. Robots are represented by the black dots and they are on hexagonal formation. Each neighbour of a robot is distant by d, so $\triangle ABC$ is equilateral. Thus, $\theta + \psi = \pi/3$.

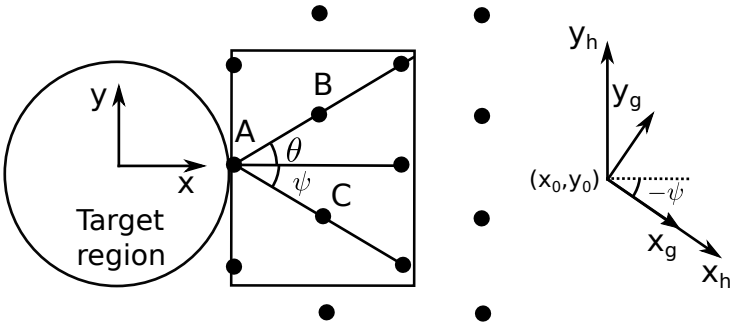

Figure S4. The reference frames used in this proof.

Let $\psi = \pi/3 - \theta$ (because the angle of the equilateral triangle formed by neighbours is $\pi/3$, as explained in Figure S4). Accordingly, $\psi \in [0, \pi/3)$ too. The usual Euclidean coordinate space which represents the location of all robots is denoted here by (x,y) coordinates. The next coordinate space is denoted by (x_g,y_g), and it is the result of a translation of the usual Euclidean coordinate space by the position of the first robot to reach the target region at (x_0,y_0), then a rotation of $-\psi$, that is, $\begin{bmatrix} x_g \\ y_g \end{bmatrix} = \begin{bmatrix} \cos(-\psi) & -\sin(-\psi) \\ \sin(-\psi) & \cos(-\psi) \end{bmatrix} \begin{bmatrix} x - x_0 \\ y - y_0 \end{bmatrix}$. The last coordinate space is denoted by (x_h,y_h), and it is intended to represent a hexagonal grid such that the position of each robot is an integer pair.

Figure S5 shows an example of the location of robots with respect to that hexagonal grid. Robots are located in the l, m, n, p, q and r lines, which are parallel to the y_h-axis. In this example, $\psi = 0.227$ and the distance between all robots is $d = 0.5$. The distance between those parallel-to-y_h lines is $\sqrt{3}d/2$. The robots inside the rectangle $EFGH$ are counted and are indicated by red points, while blue points are robots outside the rectangle. Although the x_h-axis coincides with the x_g-axis, x_h is scaled by d.

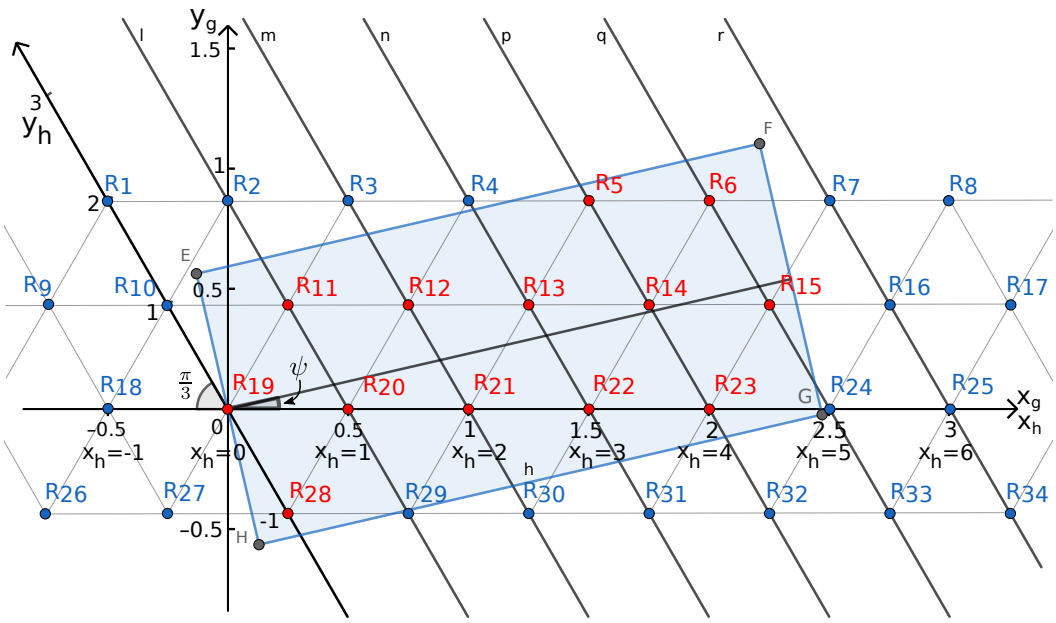

Figure S5. Example of robots in hexagonal packing formation, and the corresponding rectangular corridor which will reach the target region.

Let $(x_h, y_h) \in \mathbb{Z}^2$ be the hexagonal coordinates of a robot in this hexagonal grid space. In this figure, there is an integer grid in grey – the horizontal lines correspond to fixed integer y_h values and the inclined ones, x_h values. For example, in Figure S5 robots R_{10}, R_{11} and R_{20} respectively are at $(0,1)$, $(1,1)$ and $(1,0)$ at (x_h, y_h) coordinate system, which is equivalent to $\left(-1/4, \sqrt{3}/4\right)$, $\left(1/4, \sqrt{3}/4\right)$ and $\left(1/2, 0\right)$ on the usual two dimensional coordinate system with origin at (x_0, y_0).

A linear transformation H from a point (x_h, y_h) to (x_g, y_g) basis is obtained by knowing the result of this transformation for the standard vectors $(1,0)$ and $(0,1)$. Observing Figure S5 and having that the angle between the x-axis and y_h-axis is by definition $2\pi/3$, one gets the following mappings $(x_h, y_h) \mapsto (x_g, y_g)$: $(1,0) \mapsto (d,0)$ and $(0,1) \mapsto (d\cos(2\pi/3), d\sin(2\pi/3)) = (-\frac{d}{2}, \frac{\sqrt{3}d}{2})$ (in Figure S5 these two mappings are represented by robots R_{20} and R_{10}, respectively, with $d = 0.5$). Then,

$$\begin{bmatrix} x_g \\ y_g \end{bmatrix} = \begin{bmatrix} H\left(\begin{bmatrix} 1 \\ 0 \end{bmatrix}\right) & H\left(\begin{bmatrix} 0 \\ 1 \end{bmatrix}\right) \end{bmatrix} \begin{bmatrix} x_h \\ y_h \end{bmatrix} = \begin{bmatrix} d & -\frac{d}{2} \\ 0 & \frac{\sqrt{3}d}{2} \end{bmatrix} \begin{bmatrix} x_h \\ y_h \end{bmatrix}. \tag{S3}$$

Counting the robots inside the rectangle is the same as counting the number of integer hexagonal coordinate points lying inside it. Figure S6 shows the rectangular part with some robots in hexagonal packing, where the robots are the red dots, and the hexagonal packing is guided by the grey lines inside the rectangle based on the value of the angle ψ. The rectangle has width $vT - s$ and height $2s$. The reference frame of the hexagonal grid is rotated about the target region (Figure S4). The problem involves the rectangle $EFGH$ in a hexagonal grid (grey lines inside the rectangle) of robots (the red dots). The x_h-axis is horizontal and coincides with the x-axis. The y_h-axis forms a $2\pi/3$ angle with it. $\overline{EH}$ and $\overline{AB}$ have length $2s$ and $vT - s$, respectively. In this example, $\psi = 19\pi/180$ and $s = 1$. The angles marked with a line are equal to ψ, because the angle formed by $\overrightarrow{y_2 A}$ and the x-axis is right, as well as $\widehat{EAB}$. Accordingly, $\widehat{y_2 AB} = \pi/2 - \psi$ implies that $\widehat{EAy_2} = \psi$.

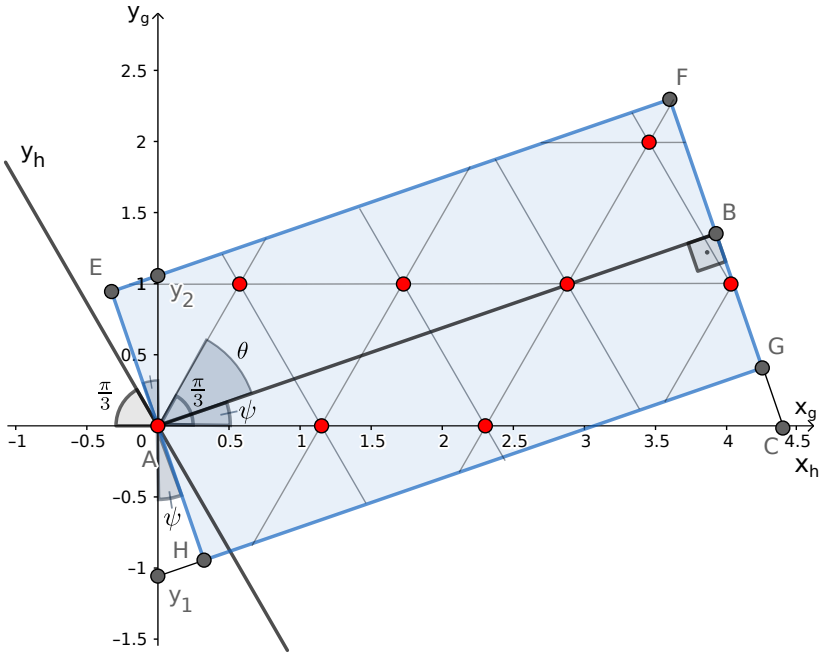

Figure S6. Example of counting robots in hexagonal packing with rotation in the reference frame.

From Figure S6,

$$2s = (y_2 - y_1)\cos(\psi),\ y_2 = \frac{s}{\cos(\psi)} \text{ and } y_1 = -\frac{s}{\cos(\psi)}. \tag{S4}$$

Consider a robot with coordinates (x_g, y_g). The four sides of the rectangle $EFGH$, $\overline{HG}$, $\overline{EF}$, $\overline{EH}$ and $\overline{FG}$, have the following equations of line: $y_g = y_1 + \tan(\psi)x_g$, $y_g = y_2 + x_g\tan(\psi)$, $y_g = \tan\left(\psi + \frac{\pi}{2}\right)x_g$ and $y_g = \tan(\psi + \frac{\pi}{2})\left(x_g - \frac{vT-s}{\cos(\psi)}\right)$, respectively. The term $\frac{vT-s}{\cos(\psi)}$ in the last equation arises because of the length of $\overline{AC}$, which is the hypotenuse of $\triangle ABC$ whose side $\overline{AB}$ measures vT. Knowing that $\tan\left(\psi + \frac{\pi}{2}\right) = -\cot(\psi)$, the equations below are all true for a robot at (x_g, y_g) to be inside or on the boundary of the previously defined rectangle,

$$\begin{aligned} &y_g \geq y_1 + x_g\tan(\psi),\ y_g \leq y_2 + x_g\tan(\psi),\ -x_g \leq \tan(\psi)y_g, \text{ and} \\ &-\left(x_g - \frac{vT-s}{\cos\psi}\right) \geq \tan(\psi)y_g. \end{aligned} \tag{S5}$$

Now take the minimum and maximum y_h value for each parallel-to-y_h line depending on the x_h value. Using (S3) for converting (S5) to x_h and y_h coordinate system, i.e., hexagonal coordinates, one obtains for $\overline{HG}$ and $\overline{EF}$ $\left(\frac{\sqrt{3}}{2} + \frac{1}{2}\tan(\psi)\right)y_h - \tan(\psi)x_h \geq \frac{y_1}{d}$ and $\left(\frac{\sqrt{3}}{2} + \frac{1}{2}\tan(\psi)\right)y_h - \tan(\psi)x_h \leq \frac{y_2}{d}$. Hence, $\frac{y_1}{d} \leq \left(\frac{\sqrt{3}}{2} + \frac{1}{2}\tan\psi\right)y_h - \tan(\psi)x_h \leq \frac{y_2}{d} \Leftrightarrow$

$$\frac{\frac{2y_1}{d} + 2\tan(\psi)x_h}{\sqrt{3} + \tan(\psi)} \leq y_h \leq \frac{\frac{2y_2}{d} + 2\tan(\psi)x_h}{\sqrt{3} + \tan(\psi)}. \tag{S6}$$

Analogously, but considering $\overline{EH}$ and $\overline{FG}$,

$$-x_h \leq \left(\tan(\psi)\frac{\sqrt{3}}{2} - \frac{1}{2}\right)y_h \text{ and } \left(\tan(\psi)\frac{\sqrt{3}}{2} - \frac{1}{2}\right)y_h \leq \frac{vT-s}{d\cos(\psi)} - x_h. \tag{S7}$$

Based on the sign of $\left(\tan(\psi)\frac{\sqrt{3}}{2} - \frac{1}{2}\right)$ and excluding the null case (when $\psi = \pi/6$), there are two different inequalities over y_h. Assuming $\psi \in [0, \pi/3)$, $\left(\tan(\psi)\frac{\sqrt{3}}{2} - \frac{1}{2}\right) > 0 \Leftrightarrow \tan(\psi)\frac{\sqrt{3}}{2} > \frac{1}{2} \Leftrightarrow \tan(\psi) > \frac{1}{\sqrt{3}} \Leftrightarrow \psi > \pi/6$. Thus, from (S7),

$$\begin{aligned} \frac{-2x_h}{\sqrt{3}\tan(\psi) - 1} \leq y_h \leq \frac{\frac{2(vT-s)}{d\cos(\psi)} - 2x_h}{\sqrt{3}\tan(\psi) - 1}, \text{ if } \psi > \pi/6, \\ \frac{\frac{2(vT-s)}{d\cos(\psi)} - 2x_h}{\sqrt{3}\tan(\psi) - 1} \leq y_h \leq \frac{-2x_h}{\sqrt{3}\tan(\psi) - 1}, \text{ if } \psi < \pi/6. \end{aligned} \tag{S8}$$

(S6) and (S8) restrict the value of y_h depending on the value of x_h by the relation

$$\begin{aligned} &\max\left(\frac{\frac{2y_1}{d} + 2\tan(\psi)x_h}{\sqrt{3} + \tan(\psi)}, \frac{-2x_h}{\sqrt{3}\tan(\psi) - 1}\right) \leq y_h \\ &\leq \min\left(\frac{\frac{2y_2}{d} + 2\tan(\psi)x_h}{\sqrt{3} + \tan(\psi)}, \frac{\frac{2(vT-s)}{d\cos(\psi)} - 2x_h}{\sqrt{3}\tan(\psi) - 1}\right), \text{ if } \psi > \pi/6, \\ &\max\left(\frac{\frac{2y_1}{d} + 2\tan(\psi)x_h}{\sqrt{3} + \tan(\psi)}, \frac{\frac{2(vT-s)}{d\cos(\psi)} - 2x_h}{\sqrt{3}\tan(\psi) - 1}\right) \leq y_h \\ &\leq \min\left(\frac{\frac{2y_2}{d} + 2\tan(\psi)x_h}{\sqrt{3} + \tan(\psi)}, \frac{-2x_h}{\sqrt{3}\tan(\psi) - 1}\right), \text{ if } \psi < \pi/6. \end{aligned} \tag{S9}$$

Using hexagonal coordinates the position of each robot is represented by a pair of integers. Then, assuming x_h and y_h integers, (S9) becomes $\lceil Y_1^R(x_h) \rceil \leq y_h \leq \lfloor Y_2^R(x_h) \rfloor$, for

$$Y_1^R(x_h) = \begin{cases} \max\left(\frac{\sin(\psi)x_h - \frac{s}{d}}{\cos\left(\frac{\pi}{6} - \psi\right)}, \frac{-\cos(\psi)x_h}{\sin\left(\psi - \frac{\pi}{6}\right)}\right), & \text{if } \psi > \pi/6, \\ \max\left(\frac{\sin(\psi)x_h - \frac{s}{d}}{\cos\left(\frac{\pi}{6} - \psi\right)}, \frac{\frac{vT-s}{d} - \cos(\psi)x_h}{\sin\left(\psi - \frac{\pi}{6}\right)}\right), & \text{if } \psi < \pi/6, \\ \frac{x_h}{2} - \frac{s}{d}, & \text{if } \psi = \pi/6, \end{cases} \tag{S10}$$

$$Y_2^R(x_h) = \begin{cases} \min\left(\frac{\sin(\psi)x_h + \frac{s}{d}}{\cos\left(\frac{\pi}{6} - \psi\right)}, \frac{\frac{vT-s}{d} - \cos(\psi)x_h}{\sin\left(\psi - \frac{\pi}{6}\right)}\right), & \text{if } \psi > \pi/6, \\ \min\left(\frac{\sin(\psi)x_h + \frac{s}{d}}{\cos\left(\frac{\pi}{6} - \psi\right)}, \frac{-\cos(\psi)x_h}{\sin\left(\psi - \frac{\pi}{6}\right)}\right), & \text{if } \psi < \pi/6, \\ \frac{x_h}{2} + \frac{s}{d}, & \text{if } \psi = \pi/6. \end{cases} \tag{S11}$$

The simplifications above used (S4), $\cos\left(\frac{\pi}{6} - \psi\right) = \frac{\sqrt{3}}{2}\cos(\psi) + \frac{1}{2}\sin(\psi)$ and $\sin\left(\psi - \frac{\pi}{6}\right) = \frac{\sqrt{3}}{2}\sin(\psi) - \frac{1}{2}\cos(\psi)$.

Now it is obtained the possible integer values for the x_h-axis which are inside the rectangle $EFGH$, that is, it is counted the number of lines parallel with the y_h-axis that intersect the rectangle for x_h integer values. Let n_l be the number of such parallel lines. Consider $n_l = n_l^- + n_l^+$, such that n_l^- is the number of lines parallel to the y_h-axis whose intersection with the x_h-axis is a point $(i, 0)$ for $i < 0$ and $i \in \mathbb{Z}$, and n_l^+ is similar but for non-negative integer i. For example, Figure S5 has $n_l^- = 0$ and $n_l^+ = 6$ (it is marked below the values of the points over the x-axis the equivalent over x_h-axis, in order to aid enumerating them). Note that the point $(i, 0)$ may be outside of the rectangle, but it will still be counted if there are integer (i, y_h) coordinates inside the rectangle. The next lemma shows how to compute n_l^+ and n_l^- to aid in this proof development.

Lemma S1. *On the (x_h, y_h) coordinate system, the integer values for x_h robot coordinates inside the rectangle EFGH are in the set $\{-n_l^-, \ldots, n_l^+ - 1\}$ with*

$$n_l^+ = \left\lfloor \frac{2(vT - s)\cos(\psi - \pi/6) + 2s\sin(|\psi - \pi/6|)}{\sqrt{3}d} + 1 \right\rfloor, \tag{S12}$$

and

$$n_l^- = \left\lfloor \frac{2s\sin(|\psi - \pi/6|)}{\sqrt{3}d} \right\rfloor. \tag{S13}$$

Proof. For getting n_l^+, it is counted how many parallel-to-y_h lines, when projected over the x-axis, are distant from each other by d on this axis and are inside the rectangle. These lines must intersect the diagonal $\overline{HF}$ of the rectangle, but commencing from the intersection between the y_h-axis and the diagonal, i.e., from B_0 in the Figure S7. In this figure, B_i is the intersection of a parallel-to-y_h line on a x_h integer coordinate and the diagonal $\overline{HF}$. The triangles AD_iC_i for any $i \in \{1, 2\}$ and ADC are similar. $\overline{AD_i}$ and $\overline{AC_i}$ have distance $i \cdot d$ and $i \cdot e$, respectively. In this example, $d = 2$ and there are three points lying over $\overline{HF}$.

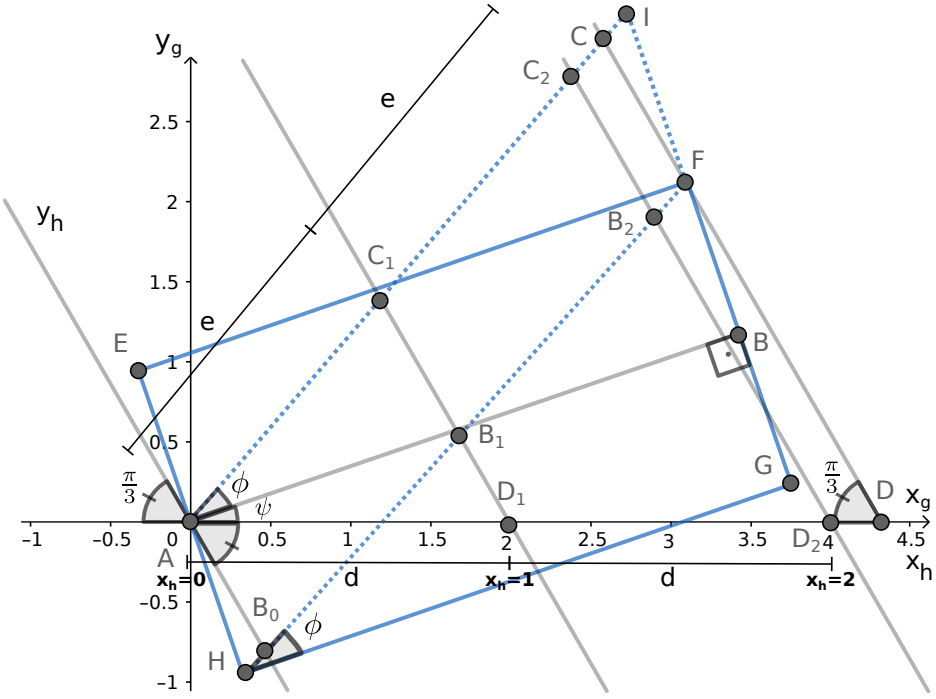

Figure S7. Counting how many points named B_i lie in the diagonal $\overline{HF}$.

Let $\phi = \arctan\left(\frac{2s}{vT - s}\right)$ be the angle of the diagonal in relation to the rectangle base. There are two cases depending on the value of ψ.

- Case $\psi \leq \frac{\pi}{6}$: from Figure S7, every line parallel to y_h is distant by d on the projection onto the x-axis. The triangles AD_iC_i for any $i \in \{1, \ldots, n_l^+ - 1\}$ and ADC are similar, $|\overline{AD_1}| = d$ and $|\overline{AC_1}| = e$, whose value is unknown for the moment. $\triangle ADC$ has angles $\widehat{CAD} = \psi + \phi$, $\widehat{ADC} = \pi/3$ and $\widehat{ACD} = \pi - \widehat{CAD} - \widehat{ADC} = 2\pi/3 - \psi - \phi$. As for every i, $\triangle AD_iC_i \sim \triangle ADC$,

$$\frac{|\overline{AC}|}{|\overline{AC_1}|} = \frac{|\overline{AD}|}{|\overline{AD_1}|} \Leftrightarrow \frac{|\overline{AC}|}{e} = \frac{|\overline{AD}|}{d}. \tag{S14}$$

As $AHFI$ is a parallelogram, $|\overline{HF}| = |\overline{AI}|$ and $|\overline{FI}| = |\overline{AH}| = s$, then $|\overline{BI}| = 2s$. Thus, $|\overline{AI}| = \sqrt{(2s)^2 + (vT - s)^2}$, because $\triangle ABI$ is right-angled. Also, by the law of sines, $\frac{|\overline{AD}|}{\sin(\widehat{ACD})} = \frac{|\overline{AC}|}{\sin(\widehat{ADC})} \Leftrightarrow$

$$\begin{aligned} |\overline{AD}| &= |\overline{AC}| \frac{\sin(\widehat{ACD})}{\sin(\widehat{ADC})} = \left(|\overline{AI}| - |\overline{CI}|\right) \frac{\sin(\widehat{ACD})}{\sin(\widehat{ADC})} \\ &= \left(|\overline{AI}| - |\overline{CI}|\right) \frac{\sin(2\pi/3 - \psi - \phi)}{\sin(\pi/3)}. \end{aligned} \tag{S15}$$

AB_0FC is a parallelogram as well, so $|\overline{AC}| = |\overline{B_0F}| = |\overline{HF}| - |\overline{HB_0}|$ and $|\overline{CI}| = |\overline{HB_0}|$. The $\triangle AB_0H$ has angles $\widehat{HAB_0} = \widehat{HAB} - \widehat{B_0AB} = \widehat{HAB} - (\widehat{B_0AD} + \widehat{DAB}) = \pi/2 - (\pi/3 + \psi) = \pi/6 - \psi$, $\widehat{AHB_0} = \widehat{AHG} - \widehat{FHG} = \pi/2 - \phi$ and $\widehat{HB_0A} = \pi - \widehat{HAB_0} - \widehat{AHB_0} = \pi/3 + \psi + \phi$. By the law of sines, $|\overline{HB_0}| = \frac{\sin(\widehat{HAB_0})|\overline{AH}|}{\sin(\widehat{HB_0A})} = \frac{\sin(\pi/6 - \psi)s}{\sin(\pi/3 + \psi + \phi)}$. Hence, from (S15), $|\overline{AD}| = \left(|\overline{AI}| - |\overline{CI}|\right) \frac{\sin(2\pi/3 - \psi - \phi)}{\sin(\pi/3)}$, thus

$$|\overline{AD}| = \frac{2\cos(\pi/6 - \psi)(vT - s) + 2s\sin(\pi/6 - \psi)}{\sqrt{3}} \tag{S16}$$

Above it was used $\sin(2\pi/3 - \psi) = \cos(\pi/6 - \psi)$, $\cos(2\pi/3 - \psi) = -\sin(\pi/6 - \psi)$, $\sin(2\pi/3 - \psi - \phi) = \sin(\pi/3 + \psi + \phi)$, $\sin(2\pi/3 - \psi - \phi) = \sin(2\pi/3 - \psi)\cos(\phi) - \cos(2\pi/3 - \psi)\sin(\phi)$, $\sin(\arctan(y/x)) = \frac{y}{\sqrt{x^2+y^2}}$, and $\cos(\arctan(y/x)) = \frac{x}{\sqrt{x^2+y^2}}$. Therefore, the number of lines parallel to the y_h-axis intersecting $\overline{B_0F}$ for integer x_h values is $n_l^+ = \left\lfloor \frac{|\overline{B_0F}|}{e} + 1 \right\rfloor = \lfloor \frac{2\cos(\pi/6 - \psi)(vT - s) + 2s\sin(\pi/6 - \psi)}{\sqrt{3}d} + 1 \rfloor$ by using (S14) and (S16).

- Case $\psi > \frac{\pi}{6}$: Figure S8 shows this case. The triangles AD_iC_i for any $i \in \{1, 2\}$ and ADC are similar. $\overline{AD_i}$ and $\overline{AC_i}$ have distance $i \cdot d$ and $i \cdot e$, respectively. In this example, $d = 2$ and there are three points lying over $\overline{EG}$. Observe that when $\psi > \frac{\pi}{6}$, $\overline{EA}$ is on the left side of the y_h-axis. Also, note that it is being considered now the diagonal $\overline{EG}$, because the y_h-axis does not intersect the diagonal $\overline{HF}$ for these values of ψ. Then, one has to consider $\overline{B_0G}$ to count n_l^+. Additionally, $|B_0G| = |AC|$, due to the AB_0GC parallelogram properties. As in the previous case, for $i \in \{1, \ldots, n_l^+ - 1\}$, $\triangle AD_iC_i \sim \triangle ADC$, $\widehat{CAD} = \widehat{BAD} - \widehat{BAC} = \psi - \phi$, $\widehat{ADC} = \pi/3$, $\widehat{ACD} = \pi - \widehat{CAD} - \widehat{ADC} = 2\pi/3 - \psi + \phi$, and $\frac{|\overline{B_0G}|}{e} = \frac{|\overline{AC}|}{e} = \frac{|\overline{AD}|}{d}$, by the similarity of these triangles as showed in the previous case. Also, $\widehat{EAB_0} = \widehat{DAE} - \widehat{DAB_0} = \psi + \pi/2 - 2\pi/3 = \psi - \pi/6$, $\widehat{B_0EA} = \widehat{FEA} - \widehat{FEB_0} = \pi/2 - \phi$, $\widehat{EB_0A} = \pi - \widehat{B_0EA} - \widehat{EAB_0} = \pi - (\pi/2 - \phi) - (\psi - \pi/6) = 2\pi/3 + \phi - \psi$. Thus, by the law of sines, $\frac{|\overline{B_0E}|}{\sin(\widehat{EAB_0})} = \frac{|\overline{EA}|}{\sin(\widehat{EB_0A})} \Leftrightarrow |\overline{B_0E}| = \frac{s\sin(\widehat{EAB_0})}{\sin(\widehat{EB_0A})} = \frac{s\sin(\psi - \pi/6)}{\sin(2\pi/3 + \phi - \psi)}$. $EAIG$ and B_0ACG are parallelograms sharing the points G and A, so $|\overline{B_0E}| = |\overline{CI}|$. By following similar steps as before, $n_l^+ = \left\lfloor \frac{2\cos(\pi/6 - \psi)(vT - s) + 2s\sin(\psi - \pi/6)}{\sqrt{3}d} + 1 \right\rfloor$. This time $\sin(2\pi/3 - \psi) = \cos(\psi - \pi/6)$ and $\cos(2\pi/3 - \psi) = \sin(\psi - \pi/6)$ was used.

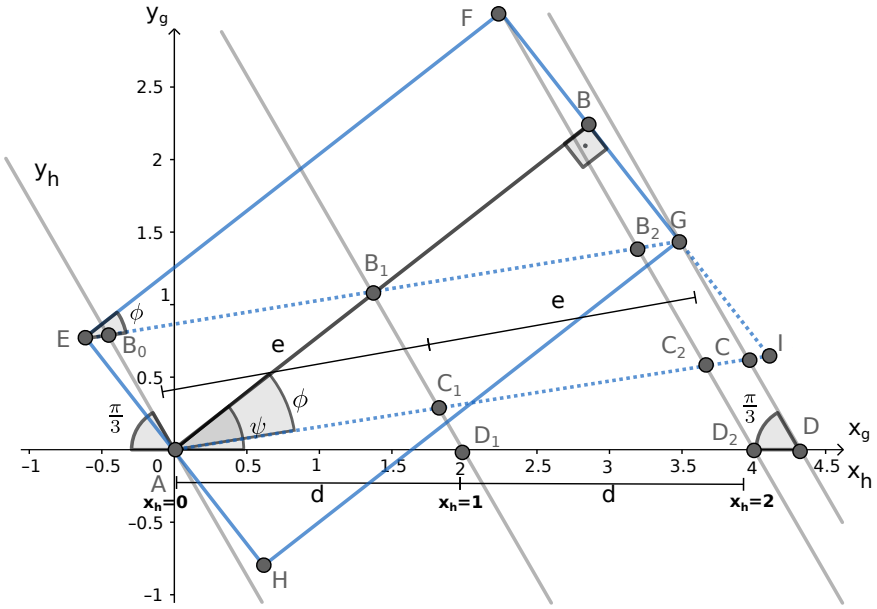

Figure S8. Counting how many points named B_i lie in the diagonal $\overline{EG}$.

For the final result on (S12), one can simplify it using the fact that when $\psi \leq \pi/6$, $\sin(|\psi - \pi/6|) = \sin(\pi/6 - \psi)$, otherwise, $\sin(|\psi - \pi/6|) = \sin(\psi - \pi/6)$.

For n_l^-, it is also calculated how many lines parallel to the y_h-axis projected over the x-axis are distant from each other by d on this axis and are inside the rectangle. However, consider only those on the left side of the point A, i.e., commencing from the one whose intersection with the x-axis is at $(-d, 0)$, equivalently, $(-1, 0)$ on the (x_h, y_h) coordinate system. Also, there are two cases here.

- Case $\psi \leq \pi/6$: Figure S9 shows the $\triangle HIA$ on the left side of the rectangle $EFGH$. The pink line on the left side is an example of one satisfying Lemma S3, while the one on the right side, Lemma S4. The triangles ACE, HIA, BMG and BNF are congruent, because their respective angles are equal – due to parallelism – and $|\overline{EA}| = |\overline{AH}| = |\overline{GB}| = |\overline{FB}| = s$. In this example, except for $\overleftrightarrow{JH}, \overleftrightarrow{EC}, \overleftrightarrow{MG}, \overleftrightarrow{BL}$ and $\overleftrightarrow{FD}$, the lines parallel-to-y_h are distant by d on the projection over the x-axis and can have robots on them. As the robots are over the parallel-to-y_h lines distant by d on the projection over the x-axis, the goal is to know how many parallel lines intersect $\overline{HI}$ (equivalently, how many such lines intersect $\overline{JA}$ due to parallelism), excluding $\overleftrightarrow{AI}$ (because it was already counted on n_l^+). Thus, $n_l^- = \left\lfloor \frac{|HI|}{d} \right\rfloor$. It is known that $|\overline{AH}| = s, \widehat{H} = \pi/2 + \psi, \widehat{I} = \pi/3$ and $\widehat{A} = \pi - \widehat{I} - \widehat{H} = \pi - \pi/3 - (\pi/2 + \psi) = \pi/6 - \psi$. By the law of sines on the angles opposite to the sides $\overline{AH}$ and $\overline{HI}$, results the following

$$|HI| = \frac{|AH| \sin(\widehat{A})}{\sin(\widehat{I})} = \frac{s \sin\left(\frac{\pi}{6} - \psi\right)}{\sin\left(\frac{\pi}{3}\right)} = \frac{2s \sin\left(\frac{\pi}{6} - \psi\right)}{\sqrt{3}}. \tag{S17}$$

Thus, $n_l^- = \left\lfloor \frac{2s \sin\left(\frac{\pi}{6} - \psi\right)}{\sqrt{3}d} \right\rfloor$.

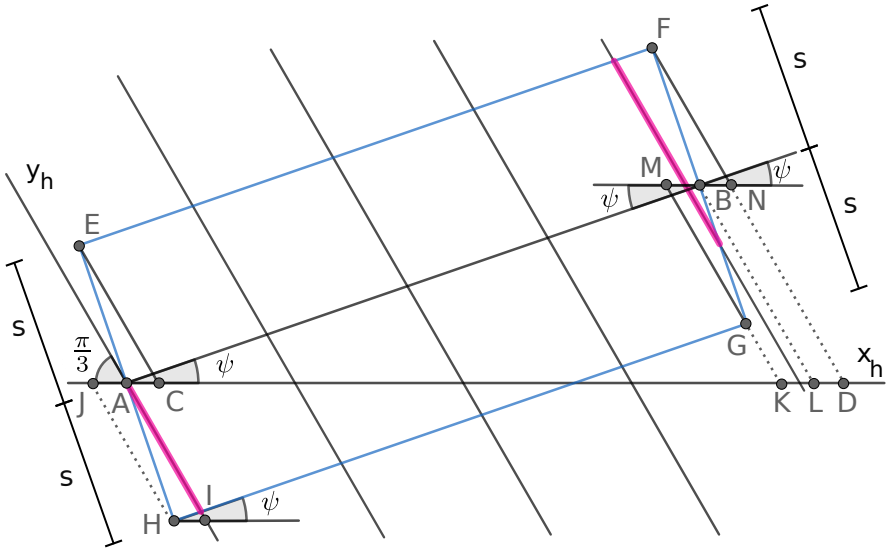

Figure S9. Triangles ACE, HIA, BMG, BNF and the rectangle $EFGH$ for $\psi \leq \pi/6$.

- Case $\psi > \pi/6$. Figure S10 illustrates this case. The side EH has an angle greater than zero with the y_h-axis. The pink line on the left side is an example of one satisfying Lemma S3, while the one on the right side, Lemma S4. The triangles AIE, HCA, FNB and BMG are congruent, because their respective angles are equal – due to parallelism – and $|\overline{EA}| = |\overline{AH}| = |\overline{GB}| = |\overline{FB}| = s$. Except for $\overleftrightarrow{EJ}$, $\overleftrightarrow{CH}$, $\overleftrightarrow{FK}$, $\overleftrightarrow{BL}$ and $\overleftrightarrow{GD}$, the lines parallel-to-y_h are distant by d on the projection over the x-axis and can have robots on them. The reasoning is similar to the previous case, but now using $\triangle EIA$. Then, $|\overline{EA}| = s, \widehat{E} = \pi/2 - \psi$, $\widehat{I} = 2\pi/3$ and $\widehat{A} = \pi - \widehat{I} - \widehat{E} = \pi - 2\pi/3 - (\pi/2 - \psi) = \psi - \pi/6$. Consequently, $n_l^- = \left\lfloor \frac{|\overline{EI}|}{d} \right\rfloor = \left\lfloor \frac{2s \sin(\psi - \frac{\pi}{6})}{\sqrt{3}d} \right\rfloor$.

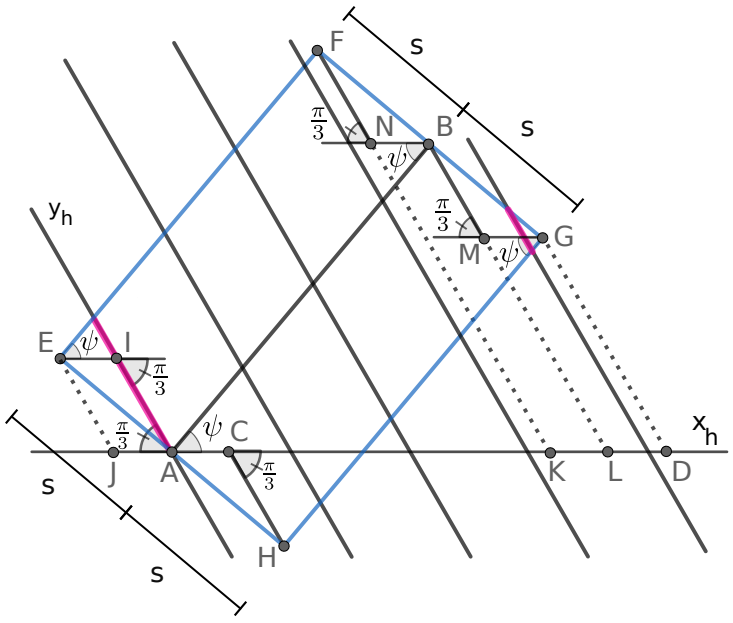

Figure S10. Triangles AIE, HCA, FNB and BMG and the rectangle $EFGH$ for $\psi > \pi/6$.

For the final result in (S13), the absolute value inside the sine function is used to combine both cases. □

The previous lemma has the calculations for the interval of an integer x_h values needed for counting the robots inside the rectangle. The next lemma presents the equation for

the number of robots at the rectangular part (N_R) ranging from these integer x_h values. Although the proposition that is now being proved gives the throughput in terms of θ, this number is first going to be calculated in terms of ψ.

Lemma S2. *For* $\psi \in [0, \pi/3)$, $N_R(T,\psi) = \sum_{x_h=-n_l^-}^{n_l^+-1} \left(\lfloor Y_2^R(x_h)\rfloor - \lceil Y_1^R(x_h)\rceil + 1\right)$. *If for some* x_h $\lfloor Y_2^R(x_h)\rfloor < \lceil Y_1^R(x_h)\rceil$, *the respective summand for this* x_h *is zero.*

Proof. By the previous lemma and knowing that the positions of the robots are integer coordinates over the hexagonal grid coordinate space, $N_R(T,\psi) = \sum_{x_h=-n_l^-}^{n_l^+-1} \left(\lfloor Y_2^R(x_h)\rfloor - \lceil Y_1^R(x_h)\rceil + 1\right)$. since (S10) and (S11) give the minimum (Y_1^R) and maximum (Y_2^R) y_h coordinates for a given x_h value such that the robot is inside the rectangle. Note that the last summation can only be used when $\lfloor Y_2^R(x_h)\rfloor \geq \lceil Y_1^R(x_h)\rceil$, otherwise a negative number of robots would be accounted. □

In special, for $\psi = \pi/6$, by (S10) and (S11),

$$N(T,\pi/6) = \sum_{x_h=0}^{\left\lfloor \frac{2(vT-s)}{\sqrt{3}d}\right\rfloor} \left(\left\lfloor \frac{\sqrt{3}y_2 + dx_h}{2d} \right\rfloor - \left\lceil \frac{\sqrt{3}y_1 + dx_h}{2d} \right\rceil + 1 \right). \tag{S18}$$

If $\psi \neq \pi/6$, each parallel-to-y_h-axis line intersects two segments of the rectangle $EFGH$. The y_h-components of the two intersections of a rectangle side and such lines are the values of $Y_1^R(x_h)$ and $Y_2^R(x_h)$ for a given x_h. Hence, the set of x_h integer values $\{-n_l^-, \ldots, n_l^+ - 1\}$ will be cut in disjoint subsets based on the max and min outcomes of (S10) and (S11). That is, $Y_1^R(x_h)$ and $Y_2^R(x_h)$, respectively; equivalently, which two sides of the rectangle the parallel-to-y_h-axis line corresponding to $(x_h, 0)$ intersects. The following lemmas describe each subset: $\{-n_l^-, \ldots, n_l^-\}$ in Lemma S3; $\{n_l^- + 1, \ldots, K' - 1\}$ in Lemma S6; $\{K', \ldots, n_l^+ - 1\}$ in Lemma S4, for an integer K' defined later.

Lemma S3. *Consider parallel-to-*y_h*-axis lines inside the rectangle* $EFGH$ *intersecting the* x_h*-axis at* $(x_h, 0)$, *for* $x_h \in \mathbb{Z}$. *The two following statements are equivalent:*

(I) *If* $\psi < \pi/6$,

$$Y_1^R(x_h) = \frac{\frac{2y_1}{d} + 2\tan(\psi)x_h}{\sqrt{3} + \tan(\psi)} \text{ and } Y_2^R(x_h) = \frac{-2x_h}{\sqrt{3}\tan(\psi) - 1}, \tag{S19}$$

and, if $\psi > \pi/6$,

$$Y_1^R(x_h) = \frac{-2x_h}{\sqrt{3}\tan(\psi) - 1} \text{ and } Y_2^R(x_h) = \frac{\frac{2y_2}{d} + 2\tan(\psi)x_h}{\sqrt{3} + \tan(\psi)}. \tag{S20}$$

(II) $x_h \in \{-n_l^-, \ldots, n_l^-\}$.

Proof. $(I) \Rightarrow (II)$: Let $\psi < \pi/6$. By (S10) and (S11), (S19) is equivalent to $\frac{\sin(\psi)x_h - \frac{s}{d}}{\cos\left(\frac{\pi}{6} - \psi\right)} \geq \frac{\frac{vT-s}{d} - \cos(\psi)x_h}{\sin\left(\psi - \frac{\pi}{6}\right)}$ and $\frac{\sin(\psi)x_h + \frac{s}{d}}{\cos\left(\frac{\pi}{6} - \psi\right)} \geq \frac{-\cos(\psi)x_h}{\sin\left(\psi - \frac{\pi}{6}\right)}$. From the second inequality, $\frac{\sin(\psi)x_h + \frac{s}{d}}{\cos\left(\frac{\pi}{6} - \psi\right)} \geq \frac{-\cos(\psi)x_h}{\sin\left(\psi - \frac{\pi}{6}\right)}$ $\Leftrightarrow x_h \leq \frac{-2s\sin\left(\psi - \frac{\pi}{6}\right)}{\sqrt{3}d} = \frac{2s\sin\left(\frac{\pi}{6} - \psi\right)}{\sqrt{3}d}$. The change of inequality sign above is due to $\cos\left(\frac{\pi}{6} - \psi\right)\sin\left(\psi - \frac{\pi}{6}\right) < 0$ for $\psi < \pi/6$. As $x_h \in \mathbb{Z}$, $x_h \leq \left\lfloor \frac{2s\sin\left(\frac{\pi}{6} - \psi\right)}{\sqrt{3}d} \right\rfloor = n_l^-$. The lower value on x_h is obtained by Lemma S1, as to be inside the rectangle $EFGH$ $x_h \geq -n_l^-$. For $\psi > \pi/6$, the same result is obtained by a similar reasoning, but without changing the inequality sign since in this case $\cos\left(\frac{\pi}{6} - \psi\right)\sin\left(\psi - \frac{\pi}{6}\right) > 0$.

$(II) \Rightarrow (I)$: From (S6), (S7) (i.e., the line equations for $\overleftrightarrow{HG}$, $\overleftrightarrow{EH}$ and $\overleftrightarrow{EF}$), (S10) and (S11) (i.e., the definitions of Y_1^R and Y_2^R), if $\psi < \pi/6$, $(x_h, Y_1^R(x_h)) \in \overleftrightarrow{HG} \Leftrightarrow Y_1^R(x_h) = \frac{\frac{2y_1}{d}+2\tan(\psi)x_h}{\sqrt{3}+\tan(\psi)}$, $(x_h, Y_2^R(x_h)) \in \overleftrightarrow{EH} \Leftrightarrow Y_2^R(x_h) = \frac{-2x_h}{\sqrt{3}\tan(\psi)-1}$, and, if $\psi > \pi/6$, $(x_h, Y_1^R(x_h)) \in \overleftrightarrow{EH} \Leftrightarrow Y_1^R(x_h) = \frac{-2x_h}{\sqrt{3}\tan(\psi)-1}$, $(x_h, Y_2^R(x_h)) \in \overleftrightarrow{EF} \Leftrightarrow Y_2^R(x_h) = \frac{\frac{2y_2}{d}+2\tan(\psi)x_h}{\sqrt{3}+\tan(\psi)}$. Then, this part is proved by showing that for all $x_h \in \{-n_l^-, \ldots, n_l^-\}$, the line parallel to the y_h-axis intercepting the point $(x_h, 0)$ intercepts both sides $\overline{EH}$ and $\overline{HG}$ (and no other), if $\psi < \pi/6$ (Figure S9), and, if $\psi > \pi/6$, both sides $\overline{EH}$ and $\overline{EF}$ (and no other) (Figure S10).

- Case $\psi < \pi/6$: Figure S9 shows the triangles HIA, ACE and BMG inside the rectangle $EFGH$. As the robots are over the parallel lines to the y_h-axis, which are distant by d when projected over the x-axis, the objective is to know how many such parallel lines intersect $\overline{HI}$ (equivalently, how many such lines intersect $\overline{JA}$ due to parallelism) or $\overline{AC}$. For such parallel lines that intersect $\overline{HI}$, Lemma S1 showed that for every $x_h \in \{-n_l^-, \ldots, -1\}$ the line parallel to y_h-axis intersecting $(x_h, 0)$ is inside the rectangle. Also, these lines intersect the sides $\overline{EH}$ and $\overline{HG}$, as any line parallel to $\overleftrightarrow{AI}$ which is on its left side intersects the sides $\overline{EH}$ and $\overline{HG}$ if it is inside the rectangle. For the case where such parallel lines intersect $\overline{AC}$, the maximum integer value, M, must be known such that these parallel lines still intersect the sides $\overline{EH}$ and $\overline{HG}$ for any $x_h \in \{0, \ldots, M\}$. Starting from point A (that is, when $x_h = 0$), $M = \left\lfloor \frac{|\overline{AC}|}{d} \right\rfloor$. It is given that $|\overline{AH}| = |\overline{EA}| = s$, $\overleftrightarrow{AI} \parallel \overleftrightarrow{EC}$, $\overleftrightarrow{HI} \parallel \overleftrightarrow{AC}$, and $\overleftrightarrow{AH} \parallel \overleftrightarrow{AE}$ (as E, A and H are collinear), then $\widehat{IHA} = \widehat{CAE}$, $\widehat{AIH} = \widehat{ECA}$, and $\widehat{HAI} = \widehat{AEC}$. Thus, $\triangle HIA \cong \triangle ACE$, then $|\overline{AC}| = |\overline{HI}|$, whose value has been previously calculated in Lemma S1, leading to $M = \left\lfloor \frac{2s\sin\left(\frac{\pi}{6}-\psi\right)}{\sqrt{3}d} \right\rfloor = n_l^-$. Hence, for any $x_h \in \{0, \ldots, n_l^-\}$, those parallel lines intersect the sides $\overline{EH}$ and $\overline{HG}$.
- Case $\psi > \pi/6$: Figure S10 illustrates this case. The reasoning is similar to the previous case, but using that $\triangle AIE \cong \triangle HCA$. As the value for $|\overline{EI}|/d$ also has been calculated in Lemma S1 for this figure, then $M = \left\lfloor \frac{2s\sin\left(\psi-\frac{\pi}{6}\right)}{\sqrt{3}d} \right\rfloor = n_l^-$. Consequently, for any $x_h \in \{-n_l^-, \ldots, n_l^-\}$, the parallel-to-$y_h$-axis line at $(x_h, 0)$ intersects the sides $\overline{EH}$ and $\overline{EF}$ in this case. □

The next lemma will define the integer K' mentioned before. This number will be compared with the integer x_h coordinate of the point $(n_l^+ - 1, 0)$ intersected by the rightmost parallel-to-y_h-axis line inside the rectangle $EFGH$. Assuming $\theta \neq \pi/6$, if this rightmost line intersects a point on the x_h-axis with an integer coordinate less than K', then no parallel-to-y_h-axis line intersects the rectangle right side $\overline{FG}$. However, if the intersection point coordinate is greater than or equal to K', then at least one parallel line crosses $\overline{FG}$.

Lemma S4. *Consider parallel-to-y_h-axis lines inside the rectangle $EFGH$ intersecting the x_h-axis at $(x_h, 0)$, for $x_h \in \mathbb{Z}$, and $K' = \left\lceil \frac{2(vT-s)\cos(\psi-\pi/6)-2s\sin(|\psi-\pi/6|)}{\sqrt{3}d} \right\rceil$. Then, the two statements below are equivalent:*

(I) *If $\psi < \pi/6$*

$$Y_1^R(x_h) = \frac{\frac{2(vT-s)}{d\cos(\psi)} - 2x_h}{\sqrt{3}\tan(\psi) - 1} \text{ and } Y_2^R(x_h) = \frac{\frac{2y_2}{d} + 2\tan(\psi)x_h}{\sqrt{3} + \tan(\psi)}, \tag{S21}$$

and, if $\psi > \pi/6$

$$Y_1^R(x_h) = \frac{\frac{2y_1}{d} + 2\tan(\psi)x_h}{\sqrt{3} + \tan(\psi)} \text{ and } Y_2^R(x_h) = \frac{\frac{2(vT-s)}{d\cos(\psi)} - 2x_h}{\sqrt{3}\tan(\psi) - 1}. \tag{S22}$$

(II) $x_h \in \{K', \ldots, n_l^+ - 1\}$.

Proof. $(I) \Rightarrow (II)$: By contrapositive, assume $x_h \notin \{K', \ldots, n_l^+ - 1\}$. By Lemma S1, there is no $x_h > n_l^+ - 1$, so $x_h < K'$. For the case of $\psi < \pi/6$, observe in Figure S9 the point K on the x_h-axis. This point corresponds to the intersection of $\overleftrightarrow{MG}$ on the x_h-axis, which is the first parallel-to-y_h-axis crossing the rectangle right side $\overline{FG}$. The point D on the x_h-axis is the projection of the point F on this axis. By (S16), $|\overline{AD}| = \frac{2\cos(\pi/6-\psi)(vT-s)+2s\sin(|\psi-\pi/6|)}{\sqrt{3}}$. Because of the parallelism, $|\overline{MN}| = |\overline{KD}|$. Due to the congruence of triangles ACE, HIA, BMG and BNF and (S17), $|\overline{BM}| = |\overline{BN}| = |\overline{HI}| = \frac{2s\sin(|\psi-\pi/6|)}{\sqrt{3}}$. Thus, $|\overline{KD}| = |\overline{MN}| = |\overline{BM}| + |\overline{BN}| = \frac{4s\sin(|\psi-\pi/6|)}{\sqrt{3}}$. Since $|\overline{AK}| = |\overline{AD}| - |\overline{KD}| = \frac{2\cos(\pi/6-\psi)(vT-s)-2s\sin(|\psi-\pi/6|)}{\sqrt{3}}$, the point K is located on the (x_h, y_h) coordinate space at $\left(\frac{2\cos(\pi/6-\psi)(vT-s)}{\sqrt{3}d} - \frac{2s\sin(|\psi-\pi/6|)}{\sqrt{3}d}, 0\right)$, as K is on the x-axis and to convert it to (x_h, y_h) coordinate space it is only needed to divide the x-coordinate by d. On the x_h-axis, the nearest point on the right of K with integer x_h is $(\lceil K \rceil, 0) = (K', 0)$. As it is assumed $x_h < K'$, no parallel-to-y_h-axis crossing a integer $(x_h, 0)$ point inside the rectangle intersects $\overline{FG}$. Thus, no such parallel line has $Y_1^R(x_h) = \frac{\frac{2(vT-s)}{d\cos(\psi)} - 2x_h}{\sqrt{3}\tan(\psi)-1}$, which is the y_h-coordinate of the intersection of this line with $\overleftrightarrow{FG}$.

In the case of $\psi > \pi/6$, using a similar argument as in Figure S10 leads to the desired result, but here $|\overline{NB}| + |\overline{MG}| = |\overline{KD}|$ and the congruence is between the triangles AIE, HCA, FNB and BMG. As it is assumed $x_h < K'$, no parallel-to-y_h-axis intersecting a integer point $(x_h, 0)$ inside the rectangle crosses $\overline{FG}$, so for such line $Y_2^R(x_h) \neq \frac{\frac{2(vT-s)}{d\cos(\psi)} - 2x_h}{\sqrt{3}\tan(\psi)-1}$.

$(II) \Rightarrow (I)$: If $x_h \in \{K', \ldots, n_l^+ - 1\}$ then the lines parallel-to-y_h-axis inside the rectangle intersecting the x_h-axis at $(x_h, 0)$ are on the right of point K or intersecting it. Hence, these lines intersect $\overline{EF}$ and $\overline{FG}$, if $\psi < \pi/6$. By applying (S6), (S7) (for the line equations for $\overleftrightarrow{EF}$ and $\overleftrightarrow{FG}$), (S10) and (S11) (for the definitions of Y_1^R and Y_2^R), (S21) is obtained. A similar argument is used in the case of $\psi > \pi/6$, but for $\overline{FG}$ and $\overline{HG}$ intersections, yielding (S22). □

The lemma below characterises when a parallel-to-y_h-axis line touches only the sides EH and FG of the rectangle. Intuitively, if this happens, a rectangle with a small width is obtained. Thus, on rectangles with a large width, no such lines are crossing the sides EH and FG, for $\psi \neq \pi/6$. This lemma will be used on the Lemma S6, for completing the disjoint subsets based on the possible max and min outcomes of Y_1^R and Y_2^R.

Lemma S5. *If* $vT - s > 2s\tan(|\psi - \frac{\pi}{6}|)$, *then there is not a* $x_h \in \{-n_l^-, \ldots, n_l^+ - 1\}$ *such that,* $Y_1^R(x_h) = \frac{\frac{2(vT-s)}{d\cos(\psi)} - 2x_h}{\sqrt{3}\tan(\psi)-1}$ *and* $Y_2^R(x_h) = \frac{-2x_h}{\sqrt{3}\tan(\psi)-1}$, *if* $\psi < \pi/6$; $Y_1^R(x_h) = \frac{-2x_h}{\sqrt{3}\tan(\psi)-1}$ *and* $Y_2^R(x_h) = \frac{\frac{2(vT-s)}{d\cos(\psi)} - 2x_h}{\sqrt{3}\tan(\psi)-1}$, *if* $\psi > \pi/6$.

Proof. This proof is by contrapositive. Assume $\psi < \pi/6$. By (S10) and (S11), there is an x_h such that $\frac{\frac{y_1}{d} + \tan(\psi)x_h}{\frac{\sqrt{3}+\tan(\psi)}{2}} \leq \frac{\frac{vT-s}{d\cos(\psi)} - x_h}{\frac{\sqrt{3}\tan(\psi)-1}{2}}$ and $\frac{\frac{y_2}{d} + \tan(\psi)x_h}{\frac{\sqrt{3}+\tan(\psi)}{2}} \geq \frac{-x_h}{\frac{\sqrt{3}\tan(\psi)-1}{2}}$. Since $\frac{\sqrt{3}\tan(\psi)-1}{2} < 0$, the signs of inequalities change, then the following implication is obtained $\frac{\frac{y_1}{d}\frac{\sqrt{3}\tan(\psi)-1}{2}}{\frac{\sqrt{3}+\tan(\psi)}{2}} - \frac{vT-s}{d\cos(\psi)} \geq -x_h - \frac{\tan(\psi)x_h\frac{\sqrt{3}\tan(\psi)-1}{2}}{\frac{\sqrt{3}+\tan(\psi)}{2}}$ and $\frac{\frac{y_2}{d}\frac{\sqrt{3}\tan(\psi)-1}{2}}{\frac{\sqrt{3}+\tan(\psi)}{2}} \leq -x_h - \frac{\tan(\psi)x_h\frac{\sqrt{3}\tan(\psi)-1}{2}}{\frac{\sqrt{3}+\tan(\psi)}{2}} \Rightarrow \frac{\frac{y_2}{d}\frac{\sqrt{3}\tan(\psi)-1}{2}}{\frac{\sqrt{3}+\tan(\psi)}{2}} \leq \frac{\frac{y_1}{d}\frac{\sqrt{3}\tan(\psi)-1}{2}}{\frac{\sqrt{3}+\tan(\psi)}{2}} - \frac{vT-s}{d\cos(\psi)}$, by the transitivity of $\leq$ under the real numbers. Also, the following equivalences is obtained $\frac{\frac{y_2}{d}\frac{\sqrt{3}\tan(\psi)-1}{2}}{\frac{\sqrt{3}+\tan(\psi)}{2}} \leq \frac{\frac{y_1}{d}\frac{\sqrt{3}\tan(\psi)-1}{2}}{\frac{\sqrt{3}+\tan(\psi)}{2}} - \frac{vT-s}{d\cos(\psi)} \Leftrightarrow vT - s \leq 2s\tan(\pi/6 - \psi)$,

due to (S4), the equalities $\tan(a+b) = \frac{\tan(a)+\tan(b)}{1-\tan(a)\tan(b)}$, $\cot(a) = -\tan(a+\pi/2)$ and $-\tan(\pi - a) = \tan(a)$ for any real a and b.

For the case $\psi > \pi/6$, using similar arguments the same result is obtained, but the signs of inequalities are not changed due to $\frac{\sqrt{3}\tan(\psi)-1}{2} > 0$ in this case. The conclusion is reached after combining the two cases using absolute values inside the tangent. □

The next lemma completes the properties of $N_R(T,\psi)$ that are useful for calculating its limit when T tends to infinity.

Lemma S6. *Let* $K' = \left\lceil \frac{2(vT-s)\cos(\psi-\pi/6)-2s\sin(|\psi-\pi/6|)}{\sqrt{3}d} \right\rceil$. *If* $vT - s > 2s\tan(|\psi - \pi/6|)$, *then* $x_h \in \{n_l^- + 1, \ldots, K' - 1\}$ *if and only if* $Y_1^R(x_h) = \frac{\frac{y_1}{d}+\tan(\psi)x_h}{\frac{\sqrt{3}+\tan(\psi)}{2}}$ *and* $Y_2^R(x_h) = \frac{\frac{y_2}{d}+\tan(\psi)x_h}{\frac{\sqrt{3}+\tan(\psi)}{2}}$.

Proof. Excluding the case when $\psi = \pi/6$, (S10) and (S11) give four combinations of possible outcomes for the values of $Y_1^R(x_h)$ and $Y_2^R(x_h)$ based on the results of min and max. When $vT - s > 2s\tan(|\psi - \pi/6|)$, by Lemma S5, there is not the case when they are on the sides EH and FG. For the given values of x_h on the hypothesis, neither Lemma S3 nor Lemma S4 applies, excluding other two combinations of results for $Y_1^R(x_h)$ and $Y_2^R(x_h)$. Finally, Lemma S1 shows that every parallel-to-y_h-axis line crosses the x_h-axis at $(x_h, 0)$ for $x_h \in \{-n_l^-, \ldots, n_l^+ - 1\}$, so the remaining combination yields the desired equivalence. □

Now the calculation of $N_S(T,\theta)$ is presented. Here θ is being used instead of $\psi = \pi/3 - \theta$ for easiness of presentation. Denote (l_x, l_y) the position of the last robot inside a rectangle of width $vT - s$ and height $2s$ whose left side is at (x_0, y_0). Here *last* means the robot with highest x coordinate value. However, if two robots have the same x coordinate value, take the robot whose y coordinate is nearer to y_0. Let Z be the set of robot positions inside the rectangle above for $vT - s > 0$.

Lemma S7. *Let* $c_x = x_0 + vT - s$, *and* $(l_x, l_y) = \operatorname{argmin}_{(x,y)\in Z} |vT - s + x_0 - x| + |y_0 - y|$ *if* $T > \frac{s}{v}$, *otherwise,* $(l_x, l_y) = (x_0, y_0)$. *Then,* $N_S(T,\theta) = \sum_{x_h=B}^{U} \left(\lfloor Y_2^S(x_h) \rfloor - \lceil Y_1^S(x_h) \rceil + 1\right)$, *for* $\lfloor Y_2^S(x_h) \rfloor \geq \lceil Y_1^S(x_h) \rceil$ *(if for some* x_h $\lfloor Y_2^S(x_h) \rfloor < \lceil Y_1^S(x_h) \rceil$, *assume the respective summand for this* x_h *being zero),*

$$B = \begin{cases} \left\lceil \dfrac{2(\sin(\pi/3-\theta)(c_x - l_x) + \cos(\pi/3-\theta)(y_0 - l_y - s))}{\sqrt{3}d} \right\rceil, & \text{if } T > \dfrac{s}{v}, \\ \left\lceil -\dfrac{2\sqrt{2svT - (vT)^2}}{\sqrt{3}d} \sin\left(\theta + \dfrac{\pi}{6}\right) \right\rceil, & \text{otherwise,} \end{cases} \tag{S23}$$

if $T > \frac{s}{v}$ *or* $\arctan\left(\frac{\frac{s}{2} - \sin(\theta)(vT-s)}{\frac{\sqrt{3}s}{2} + \cos(\theta)(vT-s)}\right) \leq \frac{\pi}{2} - \theta$,

$$U = \left\lfloor \frac{2(\sin(\pi/3-\theta)(c_x - l_x) + \cos(\pi/3-\theta)(y_0 - l_y) + s)}{\sqrt{3}d} \right\rfloor, \tag{S24}$$

otherwise,

$$U = \left\lfloor \frac{2\sqrt{2svT - (vT)^2}}{\sqrt{3}d} \cos\left(\theta - \frac{\pi}{3}\right) \right\rfloor. \tag{S25}$$

Also, $Y_1^S(x_h) = \frac{dx_h - C_{-\theta,x} + \sqrt{3}C_{-\theta,y} - \sqrt{\Delta(x_h)}}{2d}$, $Y_2^S(x_h) = \min(L(x_h), C_2(x_h)) - 1$, *if* $\min(L(x_h), C_2(x_h)) = \lfloor L(x_h) \rfloor$ *and* $T > \frac{s}{v}$, *otherwise,* $Y_2^S(x_h) = \min(L(x_h), C_2(x_h))$, *for* $C_{-\theta} = \begin{bmatrix} \cos(-\theta) & -\sin(-\theta) \\ \sin(-\theta) & \cos(-\theta) \end{bmatrix} \begin{bmatrix} c_x - l_x \\ y_0 - l_y \end{bmatrix}$, $\Delta(x_h) = 4s^2 - \left(\sqrt{3}(dx_h - C_{-\theta,x}) - C_{-\theta,y}\right)^2$, $C_2(x_h) =$

$\frac{dx_h - C_{-\theta,x} + \sqrt{3}C_{-\theta,y} + \sqrt{\Delta(x_h)}}{2d}$, *and* $L(x_h) = \frac{\sin\left(\frac{\pi}{2}-\theta\right)(dx_h - C_{-\theta,x}) + \cos\left(\frac{\pi}{2}-\theta\right)C_{-\theta,y}}{d\sin\left(\frac{5\pi}{6}-\theta\right)}$, *if* $T > \frac{s}{v}$, *otherwise,* $L(x_h) = \frac{\sin\left(\frac{\pi}{2}-\theta\right)x_h}{\sin\left(\frac{5\pi}{6}-\theta\right)}$.

Proof. Assume $T > \frac{s}{v}$, as shown in Figure S3 (III). The robots are located in the usual Euclidean space. However, instead of it, this proof uses a similar coordinate system transformation for positioning the robots in a hexagonal grid with integer coordinates, similarly to how it was performed in the rectangular part. As in the previous lemmas, call this coordinate system space coordinates (x_h, y_h). However, here a (x_h, y_h) coordinate system is being used with a different origin and inclination.

In order to do so, first redefine a (x_g, y_g) coordinate space, that is, perform rotation by $-\theta$ on the usual Euclidean space about (l_x, l_y). The origin of the (x_g, y_g) coordinate system is at (l_x, l_y). The transformation for (x_g, y_g) coordinate system used here is similar to the depicted in the Figure S4, but here $-\theta$ and (l_x, l_y) are being used instead of $-\psi$ and (x_0, y_0), i.e., $\begin{bmatrix} x_g \\ y_g \end{bmatrix} = \begin{bmatrix} \cos(-\theta) & -\sin(-\theta) \\ \sin(-\theta) & \cos(-\theta) \end{bmatrix} \begin{bmatrix} x - l_x \\ y - l_y \end{bmatrix}$. As the coordinate space (x_g, y_g) is already translated to the point (l_x, l_y), the transformation from the new (x_h, y_h) to the new (x_g, y_g) is the same as in (S3), repeated below for convenience:

$$\begin{bmatrix} x_g \\ y_g \end{bmatrix} = \begin{bmatrix} d & -\frac{d}{2} \\ 0 & \frac{\sqrt{3}d}{2} \end{bmatrix} \begin{bmatrix} x_h \\ y_h \end{bmatrix}. \tag{S26}$$

Despite these differences, the notation (x_g, y_g) and (x_h, y_h) will be kept as before for a clean presentation.

Figure S11 shows how the semicircle with centre at $C = (c_x, c_y) = (x_0 + vT - s, y_0)$ will be after the rotation by $-\theta$ about (l_x, l_y), that is,

$$C_{-\theta} = \begin{bmatrix} \cos(-\theta) & -\sin(-\theta) \\ \sin(-\theta) & \cos(-\theta) \end{bmatrix} \begin{bmatrix} c_x - l_x \\ c_y - l_y \end{bmatrix}. \tag{S27}$$

In the space (I) in Figure S11, the robots are in the standard coordinate system and the semicircle with centre at $C = (c_x, c_y)$ has the lowest point at B'. $\overleftrightarrow{CB'}$ has angle $\frac{\pi}{2}$ with the usual x-axis, however the x_h-axis here has angle θ with it. In (II) it is rotated by $-\theta$ with (l_x, l_y) as centre of rotation. After this rotation, B', U' and C become $B'_{-\theta}$, $U'_{-\theta}$ and $C_{-\theta}$, respectively, and $\overleftrightarrow{C_{-\theta}B'_{-\theta}}$ has angle $\frac{\pi}{2} - \theta$ in relation to the x_g-axis and x_h-axis, which are now coincident lines despite their scale being different. B and U are the minimum and maximum values of the x_h-axis coordinate for a line parallel to the y_h-axis on the hexagonal grid coordinate system. Hereafter the subscript $-\theta$ is on every point presented on the usual Euclidean space to denote the corresponding point on the (x_g, y_g) coordinate space.

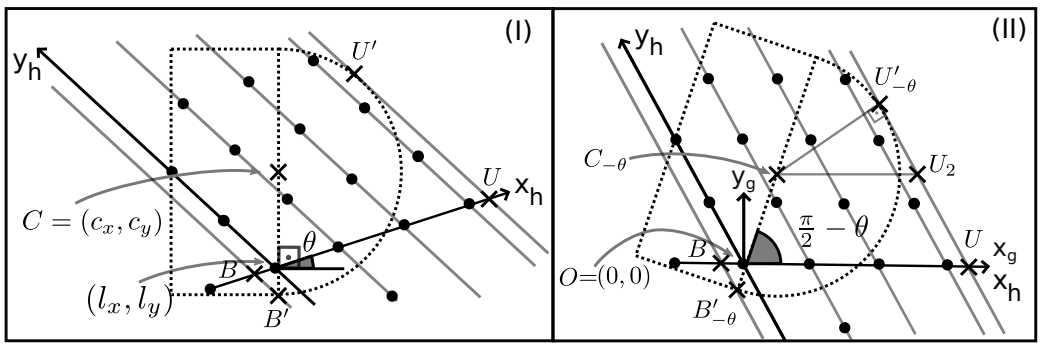

Figure S11. Semicircle for counting the robots after the rotation on the coordinate space.

The upper and lower values, U and B, of x_h lying on the semicircle are computed first. For getting the U value on the x_h-axis, draw a line parallel to the y_h-axis on the rightmost semicircle boundary at the point $U^{'}$ in order to reach the x_h-axis (Figure S11 (I)). The corresponding point on the (x_g, y_g) space is denoted by $U^{'}_{-\theta}$ (Figure S11 (II)). $U^{'}_{-\theta}$ is computed, then its x_h-value on the hexagonal grid coordinate system. $\triangle U^{'}_{-\theta}C_{-\theta}U_2$ in Figure S11 (II) has $|U^{'}_{-\theta}C_{-\theta}| = s$ and $\widehat{U^{'}_{-\theta}C_{-\theta}U_2} = \pi - \widehat{C_{-\theta}U^{'}_{-\theta}U_2} - \widehat{U^{'}_{-\theta}U_2C_{-\theta}} = \pi - \pi/2 - \pi/3 = \pi/6$. Hence, $U^{'}_{-\theta} = C_{-\theta} + s(\cos(\pi/6), \sin(\pi/6)) = \big(\cos(\theta)(c_x - l_x) + \sin(\theta)(c_y - l_y) + \frac{\sqrt{3}s}{2}, \cos(\theta)(c_y - l_y) - \sin(\theta)(c_x - l_x) + \frac{s}{2}\big)$. The inverse transformation from (S26) is

$$\begin{bmatrix} x_h \\ y_h \end{bmatrix} = \begin{bmatrix} \frac{1}{d} & \frac{1}{\sqrt{3}d} \\ 0 & \frac{2}{\sqrt{3}d} \end{bmatrix} \begin{bmatrix} x_g \\ y_g \end{bmatrix}. \tag{S28}$$

Applying the transformation of (S28) to the point $U^{'}_{-\theta}$ its x_h-axis coordinate is

$$\begin{aligned} U &= \frac{1}{d}\left(\cos(\theta)(c_x - l_x) + \sin(\theta)(c_y - l_y) + \frac{\sqrt{3}s}{2}\right) + \\ &\quad \frac{1}{\sqrt{3}d}\left(\cos(\theta)(c_y - l_y) - \sin(\theta)(c_x - l_x) + \frac{s}{2}\right) \\ &= \frac{2(\sin(\pi/3 - \theta)(c_x - l_x) + \cos(\pi/3 - \theta)(c_y - l_y) + s)}{\sqrt{3}d} \end{aligned} \tag{S29}$$

As the integer coordinate less or equal to this value is needed, the floor function is applied to yield the desired result in (S24).

For getting the B value on the x_h-axis, draw a line parallel to the y_h-axis on the lower semicircle corner at the point $B^{'}$ in order to reach the x_h-axis (Figure S11 (I)). A calculation similar to the previous paragraph is performed but using $B^{'}_{-\theta}$ (Figure S11 (II)). It is obtained $\widehat{C_{-\theta}OU} = \pi/2 - \theta$ (as this is the same angle of $\overleftrightarrow{CB'}$ with x_h-axis in Figure S11 (I) which coincides with x_g-axis in the Figure S11 (II)). Then, as the vector $C_{-\theta}B^{'}_{-\theta}$ is pointed downwards, it has negative angle with the x_g-axis, that is, $-\widehat{B_{-\theta}OU} = -(\pi - \widehat{C_{-\theta}OU}) = -(\pi - (\pi/2 - \theta)) = -\pi/2 - \theta$ with x_g-axis. Also, $\left|\overrightarrow{C_{-\theta}B^{'}_{-\theta}}\right| = s$. Consequently, $\overrightarrow{C_{-\theta}B^{'}_{-\theta}} = B^{'}_{-\theta} - C_{-\theta} = s(\cos(-\pi/2 - \theta), \sin(-\pi/2 - \theta)) \Leftrightarrow B^{'}_{-\theta} = C_{-\theta} + s(\cos(-\pi/2 - \theta), \sin(-\pi/2 - \theta)) = (\cos(\theta)(c_x - l_x) + \sin(\theta)(c_y - l_y - s), \cos(\theta)(c_y - l_y - s) - \sin(\theta)(c_x - l_x))$. Using (S28) on $B^{'}_{-\theta}$, $B = \frac{1}{d}\big(\cos(\theta)(c_x - l_x) + \sin(\theta)(c_y - l_y - s)\big) + \frac{1}{\sqrt{3}d}\big(\cos(\theta)(c_y - l_y - s) - \sin(\theta)(c_x - l_x)\big) = \frac{2(\sin(\pi/3-\theta)(c_x-l_x)+\cos(\pi/3-\theta)(c_y-l_y-s))}{\sqrt{3}d}$. Then, the ceiling function is applied on this value to get an integer coordinate greater or equal to it in order to obtain (S23) for $T > \frac{s}{v}$.

On the hexagonal grid coordinate system, for each x_h from B to U, it is needed to find the minimum and maximum y_h – namely $Y_1^S(x_h)$ and $Y_2^S(x_h)$, respectively – of a line parallel to y_h-axis intercepting the x_h-axis and lying on the semicircle. Depending on the angle of $\overleftrightarrow{C_{-\theta}B^{'}_{-\theta}}$ with the x_h-axis, the minimum and maximum y_h can be either on the semicircle arc or $\overleftrightarrow{C_{-\theta}B^{'}_{-\theta}}$. Due to $\theta \in [0, \pi/3)$, the angle of $\overleftrightarrow{C_{-\theta}B^{'}_{-\theta}}$ is in $(\frac{\pi}{6}, \frac{\pi}{2}]$. Thus, the minimum y_h value is at the semicircle arc, otherwise the minimum angle of $\overleftrightarrow{C_{-\theta}B^{'}_{-\theta}}$ would be $2\pi/3$, which is the y_h-axis angle with the x_h-axis. However, the maximum y_h value could be either on $\overleftrightarrow{C_{-\theta}B^{'}_{-\theta}}$ or on the circle, thus take the lowest, since the y_h value on the boundary of the semicircle is wanted.

Let $C_1(x_h)$ and $C_2(x_h)$ be functions that respectively return the lowest and the highest y_h value at the circle centred at $C_{-\theta}$ and radius s for a x_h coordinate value of a parallel-to-y_h-axis line assuming it intersects the circle. Then, a point (x_g, y_g) on the Euclidean

space is on that circle if $(x_g - C_{-\theta,x})^2 + (y_g - C_{-\theta,y})^2 = s^2 \Leftrightarrow \left(dx_h - \frac{dy_h}{2} - C_{-\theta,x}\right)^2 + \left(\frac{\sqrt{3}dy_h}{2} - C_{-\theta,y}\right)^2 = s^2$, by (S26).

Isolating y_h and solving the two degree polynomial it is obtained

$$y_{h_1} = C_1(x_h) = \frac{dx_h - C_{-\theta,x} + \sqrt{3}C_{-\theta,y} - \sqrt{\Delta(x_h)}}{2d} \text{ and} \tag{S30}$$

$$y_{h_2} = C_2(x_h) = \frac{dx_h - C_{-\theta,x} + \sqrt{3}C_{-\theta,y} + \sqrt{\Delta(x_h)}}{2d}, \tag{S31}$$

for $0 \leq \Delta(x_h) = 4s^2 - \left(\sqrt{3}(dx_h - C_{-\theta,x}) - C_{-\theta,y}\right)^2$. $\Delta(x_h)$ cannot be negative, otherwise the lines would not intersect this circle, contradicting the assumption.

Denote $L(x_h)$ a function that returns the y_h component of the line $\overleftrightarrow{C_{-\theta}B_{-\theta}}$ for a given x_h. The $\overleftrightarrow{C_{-\theta}B_{-\theta}}$ equation for a point in the space (x_g, y_g) is $\tan\left(\frac{\pi}{2} - \theta\right) = \frac{y_g - C_{-\theta,y}}{x_g - C_{-\theta,x}} \Rightarrow L(x_h) = y_h = \frac{\sin\left(\frac{\pi}{2} - \theta\right)(dx_h - C_{-\theta,x}) + \cos\left(\frac{\pi}{2} - \theta\right)C_{-\theta,y}}{d\sin\left(\frac{5\pi}{6} - \theta\right)}$.

$Y_1^S(x_h) = C_1(x_h)$ and $Y_2^S(x_h)$ can be either $\min(L(x_h), C_2(x_h))$ or $\min(L(x_h), C_2(x_h)) - 1$. As $T > \frac{s}{v}$, there can be a number of robots inside the rectangle $N_R(T,\theta) \geq 1$. If, for some x_h, $Y'(x_h) = \min(L(x_h), C_2(x_h)) = \lfloor L(x_h) \rfloor$, then the robot on $(x_h, Y'(x_h))$ is on the line $\overleftrightarrow{C_{-\theta}B'_{-\theta}}$. As this line belongs to the rectangle, the robot was already counted by $N_R(T,\theta)$. Hence, $Y_2^S(x_h) = \min(L(x_h), C_2(x_h)) - 1$, if $\min(L(x_h), C_2(x_h)) = \lfloor L(x_h) \rfloor$ and $T > \frac{s}{v}$, otherwise, $Y_2^S(x_h) = \min(L(x_h), C_2(x_h))$.

The number of robots inside the semicircle is the number of integer coordinates (x_h, y_h) for x_h ranging from B to U and $y_h \in \left[\lceil Y_1^S(x_h) \rceil, \lfloor Y_2^S(x_h) \rfloor\right]$ for each x_h. Thus, $N_S(T,\theta) = \sum_{x_h=B}^{U}\left(\lfloor Y_2^S(x_h) \rfloor - \lceil Y_1^S(x_h) \rceil + 1\right)$. Heed that the last summation can only be used when $\lfloor Y_2^S(x_h) \rfloor \geq \lceil Y_1^S(x_h) \rceil$, otherwise a negative number of robots would be summed.

Now, assume $T \leq \frac{s}{v}$. Then, the semicircle has centre at $C = (c_x, c_y) = (x_0 - (s - vT), y_0)$ as shown in the Figure S12. In this figure, the rotation and hexagonal grid system centres are now (x_0, y_0). Notice also in (I) that $\triangle CAO$ is right with hypotenuse $\overline{CA}$ measuring s, and the horizontal cathetus $\overline{CO}$ measures $s - vT$. Now, as there is no rectangle part, consider the *last* robot of the rectangular part being the first robot to arrive at the target region, so $(l_x, l_y) = (x_0, y_0)$, and, by (S27),

$$C_{-\theta} = \begin{bmatrix} \cos(-\theta) & -\sin(-\theta) \\ \sin(-\theta) & \cos(-\theta) \end{bmatrix} \begin{bmatrix} c_x - x_0 \\ c_y - y_0 \end{bmatrix}. \tag{S32}$$

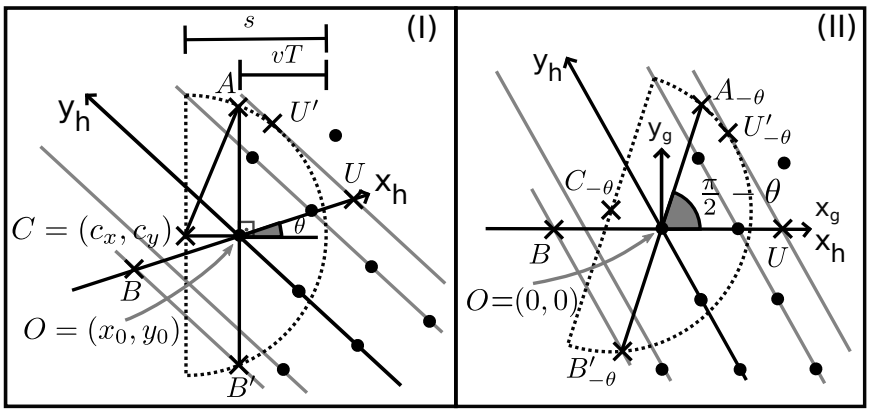

Figure S12. Similar to the coordinate spaces of Figure S11, but for $T \leq \frac{s}{v}$.

In the usual Euclidean coordinate space before the rotation about (x_0, y_0), consider the line $\overleftrightarrow{OA}$ perpendicular to the x-axis at $O = (x_0, y_0)$. This line represents the perpendicular

axis such that all the robots from it to the arc of the semicircle on its right are counted. From Figure S12 (I), $r = |\overline{AO}| = \sqrt{|\overline{CA}|^2 - |\overline{CO}|^2} = \sqrt{s^2 - (s - vT)^2} = \sqrt{2svT - (vT)^2}$.

After the rotation by $-\theta$ about the point O, the maximum value for x_h is defined by the point U. The point U is chosen depending on the angles $\widehat{U'_{-\theta}OU}$ and $\widehat{A_{-\theta}OU}$. When the angle $\widehat{U'_{-\theta}OU}$ is greater than $\widehat{A_{-\theta}OU}$, the value of U is calculated in relation to $A_{-\theta}$, because the line parallel to y_h-axis intercepting $U'_{-\theta}$ is not inside the semicircle below $\overleftrightarrow{OA_{-\theta}}$ as shown in Figure S13. It is only considered here robots inside the semicircle below the line $\overleftrightarrow{OA_{-\theta}}$, otherwise the robot on O would not be the first robot by assumption. In this case, any line parallel to y_h-axis crossing the semicircle below $\overline{OA_{-\theta}}$ must have its x_h-axis coordinate less than or equal to U, for example Q projected from P. For comparison, Figure S12 (II) illustrates an example where U is chosen as the x_h-axis intersection with the line parallel to y_h-axis at $U'_{-\theta}$. As before, for the case $T > \frac{s}{v}$ (Figure S11 (II)), the angle of $\overline{C_{-\theta}U'_{\theta}}$ in relation to x_h-axis is $\pi/6$, consequently, $U'_{-\theta} = C_{-\theta} + s\left(\cos\left(\frac{\pi}{6}\right), \sin\left(\frac{\pi}{6}\right)\right) = \left(\frac{\sqrt{3}s}{2} + \cos(\theta)(vT - s), \frac{s}{2} - \sin(\theta)(vT - s)\right)$, from (S32), and $\widehat{U'_{-\theta}OU}$ measures $\arctan\left(\frac{U'_{-\theta,y}}{U'_{-\theta,x}}\right) = \arctan\left(\frac{\frac{s}{2} - \sin(\theta)(vT-s)}{\frac{\sqrt{3}s}{2} + \cos(\theta)(vT-s)}\right)$.

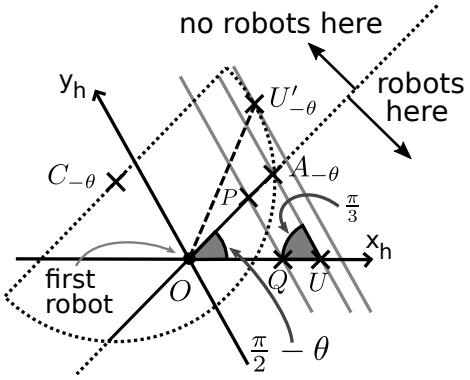

Figure S13. An example of when the angle $\widehat{U'_{-\theta}OU}$ is greater than $\widehat{A_{-\theta}OU}$.

$\widehat{A_{-\theta}OU}$ measures $\frac{\pi}{2} - \theta$, as show in Figure S12 (II). Thence, $A_{-\theta} = \left(r\cos\left(\frac{\pi}{2} - \theta\right), r\sin\left(\frac{\pi}{2} - \theta\right)\right)$. If $\arctan\left(\frac{U'_{-\theta,y}}{U'_{-\theta,x}}\right) \leq \widehat{A_{-\theta}OU} = \frac{\pi}{2} - \theta$, apply (S28) on $U'_{-\theta}$ to get its x_h-axis coordinate $U = \frac{1}{d}\left(\frac{\sqrt{3}s}{2} + \cos(\theta)(vT - s)\right) + \frac{1}{\sqrt{3}d}\left(\frac{s}{2} - \sin(\theta)(vT - s)\right) = \frac{2\sin(\pi/3-\theta)(vT-s)}{\sqrt{3}d} + \frac{2s}{\sqrt{3}d}$, followed by applying floor function to it, as the integer coordinate less or equal to this value is needed. This is the same as (S29) by using $(l_x, l_y) = (x_0, y_0)$, then (S24) also applies when $\arctan\left(\frac{\frac{s}{2} - \sin(\theta)(vT-s)}{\frac{\sqrt{3}s}{2} + \cos(\theta)(vT-s)}\right) \leq \frac{\pi}{2} - \theta$.

If $\arctan\left(\frac{U'_{-\theta,y}}{U'_{-\theta,x}}\right) > \frac{\pi}{2} - \theta$, then there are no robots to consider on the parallel lines to y_h-axis between $U'_{-\theta}$ and $A_{-\theta}$, otherwise the robot at (x_0, y_0) would not be the first to arrive at the target region. Thus, if $\arctan\left(\frac{U'_{-\theta,y}}{U'_{-\theta,x}}\right) > \frac{\pi}{2} - \theta$, the x_h-coordinate for the point $A_{-\theta}$ on the hexagonal grid space is used, that is, $U = \frac{1}{d}\left(r\cos\left(\frac{\pi}{2} - \theta\right)\right) + \frac{1}{\sqrt{3}d}\left(r\sin\left(\frac{\pi}{2} - \theta\right)\right) = \frac{2r}{\sqrt{3}d}\cos\left(\theta - \frac{\pi}{3}\right)$. then apply the floor function to yield the desired result in (S25).

Now the minimum value for an integer x_h will be found such that a parallel-to-y_h-axis line is inside the semicircle and starting from the right of $\overleftrightarrow{OA}$ or on it. For the calculation of B, from Figure S12 (II), similarly to how it was previously done, $B'_{-\theta} = O + r(\cos(-(\pi/2 + \theta)), \sin(-(\pi/2 + \theta)) = (-r\sin(\theta), -r\cos(\theta))$, and, by (S28), as B is the

x_h-coordinate of the $B_{-\theta}$, $B = \frac{1}{d}(-r\sin(\theta)) + \frac{1}{\sqrt{3}d}(-r\cos(\theta)) = -\frac{2r}{\sqrt{3}d}\sin\left(\theta + \frac{\pi}{6}\right)$. Also, apply the ceiling function to yield the desired result in (S23).

In this case, $C_1(x_h)$ and $C_2(x_h)$ are equal to (S30) and (S31), but $L(x_h)$ is different from the previous case. The line $\overleftrightarrow{OA_{-\theta}}$ for a point (x_g, y_g) in the Euclidean space is $y_g = \tan\left(\frac{\pi}{2} - \theta\right)x_g \Rightarrow L(x_h) = y_h = \frac{\sin\left(\frac{\pi}{2}-\theta\right)x_h}{\sin\left(\frac{5\pi}{6}-\theta\right)}$. □

It follows that $\lim_{T\to\infty} f_h(T,\theta) = \lim_{T\to\infty}\frac{N_R(T,\theta)}{T} + \lim_{T\to\infty}\frac{N_S(T,\theta)-1}{T}$, by Definition 2. As shown below, this limit needs only the rectangle part, because N_S is limited by a semicircle with finite radius.

Lemma S8. $\lim_{T\to\infty}\frac{N_S(T,\theta)-1}{T} = 0$.

Proof. As $T \to \infty$, $T > \frac{s}{v}$. By Lemma S7, $c_x = x_0 + vT - s$, which is the x-axis coordinate of the right side of the rectangle. The robots are distant by d, so the last robot must be at most distant by d from the point (c_x, y_0). Hence, $x_0 + vT - s - d \le l_x \le x_0 + vT - s$, and $y_0 - d \le l_y \le y_0 + d$, so $0 = c_x - (x_0 + vT - s) \le c_x - l_x \le c_x - (x_0 + vT - s - d) = d$ and $-d \le y_0 - l_y \le d$. Then, $-d \le C_{-\theta,x}, C_{-\theta,y} \le d$. Thus, $B = \left\lceil \frac{2(\sin(\pi/3-\theta)(c_x-l_x)+\cos(\pi/3-\theta)(y_0-l_y-s))}{\sqrt{3}d} \right\rceil \ge \left\lceil \frac{2(\cos(\pi/3-\theta)(-d-s))}{\sqrt{3}d} \right\rceil \ge \left\lceil \frac{-2(1+\frac{s}{d})}{\sqrt{3}} \right\rceil = \left\lceil -\frac{2}{\sqrt{3}} - \frac{s}{\sqrt{3}d} \right\rceil \ge -\frac{2}{\sqrt{3}} - \frac{s}{\sqrt{3}d}$, and $U = \left\lfloor \frac{2(\sin(\pi/3-\theta)(c_x-l_x)+\cos(\pi/3-\theta)(y_0-l_y)+s)}{\sqrt{3}d} \right\rfloor \le \left\lfloor \frac{2(\sin(\pi/3-\theta)d}{\sqrt{3}d} + \frac{\cos(\pi/3-\theta)d+s)}{\sqrt{3}d} \right\rfloor \le \left\lfloor \frac{2(2d+s)}{\sqrt{3}d} \right\rfloor \le \frac{4}{\sqrt{3}} + \frac{2s}{\sqrt{3}d}$, and for any integer $x_h \in [B, U]$, as $\Delta(x_h)$ cannot be negative, $0 \le \Delta(x_h) = 4s^2 - \left(\sqrt{3}(dx_h - C_{-\theta,x}) - C_{-\theta,y}\right)^2 \le 4s^2$, $\lceil Y_1^S(x_h)\rceil \ge Y_1^S(x_h) = \frac{dx_h - C_{-\theta,x} + \sqrt{3}C_{-\theta,y} - \sqrt{\Delta(x_h)}}{2d} \ge \frac{dx_h - d - \sqrt{3}d - 2s}{2d} = \frac{x_h - 1 - \sqrt{3}}{2} - \frac{s}{d}$, and $\lfloor Y_2^S(x_h)\rfloor \le Y_2^S(x_h) \le \min(L(x_h), C_2(x_h)) \le C_2(x_h) = \frac{dx_h - C_{-\theta,x} + \sqrt{3}C_{-\theta,y} + \sqrt{\Delta(x_h)}}{2d} \le \frac{dx_h + d + \sqrt{3}d + 2s}{2d} = \frac{x_h + 1 + \sqrt{3}}{2} + \frac{s}{d}$. Thus, $0 \le N_S(T,\theta) = \sum_{x_h=B}^{U}\left(\lfloor Y_2^S(x_h)\rfloor - \lceil Y_1^S(x_h)\rceil + 1\right) \le \sum_{x_h=B}^{U}\left(\frac{x_h+1+\sqrt{3}}{2} + \frac{s}{d} - \left(\frac{x_h-1-\sqrt{3}}{2} - \frac{s}{d}\right) + 1\right) = \sum_{x_h=B}^{U}\left(\frac{2s}{d} + \sqrt{3} + 2\right) \le \left(\frac{4}{\sqrt{3}} + \frac{2s}{\sqrt{3}d} - \left(-\frac{2}{\sqrt{3}} - \frac{s}{\sqrt{3}d}\right) + 1\right)\left(\frac{2s}{d} + \sqrt{3} + 2\right) = \left(2\sqrt{3} + \frac{\sqrt{3}s}{d} + 1\right)\left(\frac{2s}{d} + \sqrt{3} + 2\right) \Rightarrow 0 = \lim_{T\to\infty}\frac{-1}{T} \le \lim_{T\to\infty}\frac{N_S(T,\theta)-1}{T} \le \lim_{T\to\infty}\frac{1}{T}\left(\left(2\sqrt{3} + \frac{\sqrt{3}s}{d} + 1\right)\left(\frac{2s}{d} + \sqrt{3} + 2\right) - 1\right) = 0$. Hence, the result follows from the sandwich theorem. □

As $\lim_{T\to\infty}\frac{N_S(T,\theta)-1}{T} = 0$, hereafter only the limit for the number of robots inside the rectangle is calculated. By Lemmas S2 to S6, if $n_l^+ - 1 < K'$ $\lim_{T\to\infty} f_h(T,\psi) = \lim_{T\to\infty}\frac{1}{T}\sum_{x_h=-n_l^-}^{n_l^-}\left(\lfloor Y_2^R(x_h)\rfloor - \lceil Y_1^R(x_h)\rceil + 1\right) + \lim_{T\to\infty}\frac{1}{T}\sum_{x_h=n_l^-+1}^{n_l^+-1}\left(\lfloor Y_2^R(x_h)\rfloor - \lceil Y_1^R(x_h)\rceil + 1\right)$, otherwise, $\lim_{T\to\infty} f_h(T,\psi) = \lim_{T\to\infty}\frac{1}{T}\sum_{x_h=-n_l^-}^{n_l^-}\left(\lfloor Y_2^R(x_h)\rfloor - \lceil Y_1^R(x_h)\rceil + 1\right) + \lim_{T\to\infty}\frac{1}{T}\sum_{x_h=n_l^-+1}^{K'-1}\left(\lfloor Y_2^R(x_h)\rfloor - \lceil Y_1^R(x_h)\rceil + 1\right) + \lim_{T\to\infty}\frac{1}{T}\sum_{x_h=K'}^{n_l^+-1}\left(\lfloor Y_2^R(x_h)\rfloor - \lceil Y_1^R(x_h)\rceil + 1\right)$. To clarify, the third summation is zero in the case of $n_l^+ - 1 < K'$, while the second summation goes until $\min(n_l^+ - 1, K' - 1)$ in both cases. Each one will be individually solved assuming $\psi \neq \pi/6$. Later, it will be seen that the final result holds for $\psi = \pi/6$ as well. The following lemmas will be useful soon.

Lemma S9. *Assume* $\psi \neq \pi/6$. $\lim_{T\to\infty}\frac{1}{T}\sum_{x_h=-n_l^-}^{n_l^-}\left(\lfloor Y_2^R(x_h)\rfloor - \lceil Y_1^R(x_h)\rceil + 1\right) = 0$.

Proof. As for any x, $x - 1 < \lfloor x\rfloor \le x \le \lceil x\rceil < x + 1$, $\lim_{T\to\infty}\frac{1}{T}\sum_{x_h=-n_l^-}^{n_l^-}\left(Y_2^R(x_h) - Y_1^R(x_h) - 1\right) < \lim_{T\to\infty}\frac{1}{T}\sum_{x_h=-n_l^-}^{n_l^-}\left(\lfloor Y_2^R(x_h)\rfloor - \lceil Y_1^R(x_h)\rceil + 1\right) \le \lim_{T\to\infty}\frac{1}{T}\sum_{x_h=-n_l^-}^{n_l^-}\left(Y_2^R(x_h)\right.$

$-Y_1^R(x_h)+1\big)$. By Lemma S3, the first and last summations do not depend on T, so both sides have limit equal to 0. By the sandwich theorem, the result is obtained. □

Lemma S10. *Assume* $\psi \neq \pi/6$. *For* $K' = \left\lceil \frac{2(vT-s)\cos(\psi-\pi/6)-2s\sin(|\psi-\pi/6|)}{\sqrt{3}d} \right\rceil$, $\lim_{T\to\infty} \frac{1}{T} \sum_{x_h=K'}^{n_l^+-1} \big(\lfloor Y_2^R(x_h) \rfloor - \lceil Y_1^R(x_h) \rceil + 1 \big) = 0$.

Proof. If $K' > n_l^+ - 1$, this limit is already zero, so this proof is focused on the other case. Analogously to the previous lemma,

$$\begin{aligned} &\lim_{T\to\infty} \frac{1}{T} \sum_{x_h=K'}^{n_l^+-1} \Big(Y_2^R(x_h) - Y_1^R(x_h) - 1 \Big) \\ &< \lim_{T\to\infty} \frac{1}{T} \sum_{x_h=K'}^{n_l^+-1} \Big(\lfloor Y_2^R(x_h) \rfloor - \lceil Y_1^R(x_h) \rceil + 1 \Big) \\ &\leq \lim_{T\to\infty} \frac{1}{T} \sum_{x_h=K'}^{n_l^+-1} \Big(Y_2^R(x_h) - Y_1^R(x_h) + 1 \Big). \end{aligned} \tag{S33}$$

For any constant c,

$$\lim_{T\to\infty} \frac{1}{T} \sum_{x_h=K'}^{n_l^+-1} c = 0, \tag{S34}$$

because the number of x_h indexes in the summation is limited by a finite number of integer outcomes that depends on T. In other words, the number of indexes in the above summation is $n_l^+ - K'$ such that $\frac{4s\sin(|\psi-\pi/6|)}{\sqrt{3}d} - 1 < n_l^+ - K' \leq \frac{4s\sin(|\psi-\pi/6|)}{\sqrt{3}d} + 1$. The last inequality is obtained by counting how many x_h are used in the summation and knowing that $2y - 1 < \lfloor x + y \rfloor - \lceil x - y \rceil + 1 \leq 2y + 1$ for any $x, y \in \mathbb{R}$. Thus, for any T, $n_l^+ - K'$ can only range from $\left\lceil \frac{4s\sin(|\psi-\pi/6|)}{\sqrt{3}d} \right\rceil - 1$ to $\left\lfloor \frac{4s\sin(|\psi-\pi/6|)}{\sqrt{3}d} \right\rfloor + 1$. This yields to three possible integer numbers, if $\frac{4s\sin(|\psi-\pi/6|)}{\sqrt{3}d} \in \mathbb{Z}$, or four, otherwise. Thus, a finite range of outcomes, none of them having T. Hence, for all outcomes, the limit on the left side of (S34) is zero.

Assume $\psi > \pi/6$ (for $\psi < \pi/6$ the result is the same). From Lemma S4,

$$\begin{aligned} Y_2^R(x_h) - Y_1^R(x_h) &= \frac{\frac{2(vT-s)}{d\cos(\psi)} - 2x_h}{\sqrt{3}\tan(\psi) - 1} - \frac{\frac{2y_1}{d} + 2\tan(\psi)x_h}{\sqrt{3} + \tan(\psi)} \\ &= \frac{\frac{2(vT-s)}{d\cos(\psi)}}{\sqrt{3}\tan(\psi) - 1} - \frac{\frac{2y_1}{d}}{\sqrt{3} + \tan(\psi)} - \left(\frac{2}{\sqrt{3}\tan(\psi) - 1} \right. \\ &\left. + \frac{2\tan(\psi)}{\sqrt{3} + \tan(\psi)} \right) x_h. \end{aligned} \tag{S35}$$

For the second term above, by (S34), $\lim_{T\to\infty} \sum_{x_h=K'}^{n_l^+-1} \frac{\frac{2y_1}{d}}{\sqrt{3} + \tan(\psi)} = 0$.

For the first term,

$$\begin{aligned}\sum_{x_h=K'}^{n_l^+-1}\frac{1}{T}\frac{\frac{2(vT-s)}{d\cos(\psi)}}{\sqrt{3}\tan(\psi)-1}&=\sum_{x_h=K'}^{n_l^+-1}\frac{2\left(v-\frac{s}{T}\right)}{d\cos(\psi)(\sqrt{3}\tan(\psi)-1)}\\&=\sum_{x_h=K'}^{n_l^+-1}\frac{2\left(v-\frac{s}{T}\right)}{d(\sqrt{3}\sin(\psi)-\cos(\psi))}=\sum_{x_h=K'}^{n_l^+-1}\frac{v-\frac{s}{T}}{d\sin(\psi-\pi/6)}\\&=\sum_{x_h=K'}^{n_l^+-1}\frac{v}{d\sin(\psi-\pi/6)}-\frac{1}{T}\sum_{x_h=K'}^{n_l^+-1}\frac{s}{d\sin(\psi-\pi/6)},\end{aligned}\tag{S36}$$

due to $\frac{\sqrt{3}}{2}\sin(\psi)-\frac{1}{2}\cos(\psi)=\sin(\psi-\pi/6)$. Let L be the number of terms on the summation of (S36). As discussed above, L is an integer in $\left\{\left\lceil\frac{4s\sin(|\psi-\pi/6|)}{\sqrt{3}d}\right\rceil-1,\ldots,\left\lfloor\frac{4s\sin(|\psi-\pi/6|)}{\sqrt{3}d}\right\rfloor+1\right\}$, so

$$\sum_{x_h=K'}^{n_l^+-1}\frac{1}{T}\frac{\frac{2(vT-s)}{d\cos(\psi)}}{\sqrt{3}\tan(\psi)-1}=\frac{Lv}{d\sin(\psi-\pi/6)}-\frac{1}{T}\sum_{x_h=K'}^{n_l^+-1}\frac{s}{d\sin(\psi-\pi/6)}.\tag{S37}$$

Also, $\frac{2}{\sqrt{3}\tan(\psi)-1}+\frac{2\tan(\psi)}{\sqrt{3}+\tan(\psi)}=\frac{\sqrt{3}}{2\sin(\psi-\pi/6)\cos(\psi-\pi/6)}$ as $1+\tan^2(\psi)=\sec^2(\psi)$ and $\frac{\sqrt{3}}{2}\cos(\psi)+\frac{1}{2}\sin(\psi)=\cos(\psi-\pi/6)$. Hence, for the last term in (S35),

$$\begin{aligned}&\frac{1}{T}\sum_{x_h=K'}^{n_l^+-1}\frac{\sqrt{3}}{2\sin(\psi-\pi/6)\cos(\psi-\pi/6)}x_h\\&=\frac{1}{T}\frac{\sqrt{3}}{2\sin(\psi-\pi/6)\cos(\psi-\pi/6)}\frac{(n_l^+-1+K')(n_l^+-K')}{2}\\&=\frac{\sqrt{3}LG}{4T\sin(\psi-\pi/6)\cos(\psi-\pi/6)},\end{aligned}\tag{S38}$$

for an integer $G=n_l^+-1+K'$. As $2x-1<\lfloor x+y\rfloor+\lceil x-y\rceil<2x+1$ for any $x,y\in\mathbb{R}$, $G\in\left(\frac{4(vT-s)\cos(\psi-\pi/6)}{\sqrt{3}d}-1,\frac{4(vT-s)\cos(\psi-\pi/6)}{\sqrt{3}d}+1\right)$.

For the lowest bound on G, using (S37) and (S38) $\lim_{T\to\infty}\frac{1}{T}\sum_{x_h=K'}^{n_l^+-1}\left(Y_2^R(x_h)-Y_1^R(x_h)\right)=\lim_{T\to\infty}\frac{1}{T}\sum_{x_h=K'}^{n_l^+-1}\left(\frac{\frac{2(vT-s)}{d\cos(\psi)}}{\sqrt{3}\tan(\psi)-1}-\left(\frac{2}{\sqrt{3}\tan(\psi)-1}+\frac{2\tan(\psi)}{\sqrt{3}+\tan(\psi)}\right)x_h\right)=\lim_{T\to\infty}\left(\frac{Lv}{d\sin(\psi-\pi/6)}-\frac{\sqrt{3}L\left(\frac{4(vT-s)\cos(\psi-\pi/6)}{\sqrt{3}d}-1\right)}{4T\sin(\psi-\pi/6)\cos(\psi-\pi/6)}-\frac{1}{T}\sum_{x_h=K'}^{n_l^+-1}\frac{s}{d\sin(\psi-\pi/6)}\right)=\lim_{T\to\infty}\left(\frac{\sqrt{3}L}{4T\sin(\psi-\pi/6)\cos(\psi-\pi/6)}-\frac{1}{T}\sum_{x_h=K'}^{n_l^+-1}\frac{s}{d\sin(\psi-\pi/6)}\right)=0$, due to (S34) on the second term and, as $L\in\left\{\left\lceil\frac{4s\sin(|\psi-\pi/6|)}{\sqrt{3}d}\right\rceil-1,\ldots,\left\lfloor\frac{4s\sin(|\psi-\pi/6|)}{\sqrt{3}d}\right\rfloor+1\right\}$, no element in this finite set has the term T.

For the highest bound on G, the same limit is obtained. Hence, by the sandwich theorem applied on the results for both bounds of G,

$$\lim_{T\to\infty}\frac{1}{T}\sum_{x_h=K'}^{n_l^+-1}\left(Y_2^R(x_h)-Y_1^R(x_h)\right)=0.\tag{S39}$$

Using (S39) and (S34) on the bounds of (S33) and the sandwich theorem again concludes with the desired value. □

Lemma S11. *Assume* $\psi\neq\pi/6$. $\lim_{T\to\infty}\frac{1}{T}\sum_{x_h=n_l^-+1}^{\min(n_l^+-1,K'-1)}\left(\lfloor Y_2^R(x_h)\rfloor-\lceil Y_1^R(x_h)\rceil+1\right)$ *exists and is bounded by* $\left(\frac{4vs}{\sqrt{3}d^2}-\frac{2v\cos(\psi-\pi/6)}{\sqrt{3}d},\frac{4vs}{\sqrt{3}d^2}+\frac{2v\cos(\psi-\pi/6)}{\sqrt{3}d}\right]$.

Proof. The next lemmas will be useful for proving this lemma.

Lemma S12. *For any* $a, b > 0, a\lfloor x \rfloor - b\lfloor y \rfloor < ax - by + a + b.$

Proof. As mentioned before, by the definition of floor function $\lfloor x \rfloor = x - frac(x)$, where $frac$ is the function that returns the fractional part of the number x, such that $0 \leq frac(x) < 1$ [3], $a\lfloor x \rfloor - b\lfloor y \rfloor = ax - afrac(x) - by + bfrac(y) < ax - by + b - afrac(x) < ax - by + b + a$ because $frac(y) < 1$ and $-afrac(x) \leq 0 < a$. □

Lemma S13. *Let* $c, d, A_1, B_1, A_2, B_2 \in \mathbb{R}$, $c > 0$ *and* $I_1 \in \mathbb{Z}$. *Then,* $\lim_{n\to\infty} \sum_{i=I_1+1}^{\lfloor cn+d \rfloor} (frac(-(A_1 i + B_1)) + frac(A_2 i + B_2))/n$ *exists*

Proof. For convergence, it is shown that for $R(i) = frac(-(A_1 i + B_1)) + frac(A_2 i + B_2)$, $(a_n)_{n\in\mathbb{N}^*} = \left(\sum_{i=I_1+1}^{\lfloor cn+d \rfloor} \frac{R(i)}{n}\right)_{n\in\mathbb{N}^*}$ is a Cauchy sequence. Take $\epsilon > 0$ and choose $N > \frac{4|I_1-d+1|}{\epsilon}$. Let $n, m \in \mathbb{N}^*$ and $n > m > N$. Then, $|a_n - a_m| = |\sum_{i=I_1+1}^{\lfloor cn+d \rfloor} \frac{R(i)}{n} - \sum_{i=I_1+1}^{\lfloor cm+d \rfloor} \frac{R(i)}{m}| = |\frac{1}{nm}\left(m\sum_{i=I_1+1}^{\lfloor cn+d \rfloor} R(i) - n\sum_{i=I_1+1}^{\lfloor cm+d \rfloor} R(i)\right)| = |\frac{1}{nm}\left(m\sum_{i=\lfloor cm+d \rfloor+1}^{\lfloor cn+d \rfloor} R(i) + (m-n)\sum_{i=I_1+1}^{\lfloor cm+d \rfloor} R(i)\right)| < \frac{2}{|nm|}|m(\lfloor cn + d \rfloor - (\lfloor cm + d \rfloor + 1) + 1) + (m-n)(\lfloor cm + d \rfloor - (I_1 + 1) + 1)| = \frac{2}{|nm|}|m\lfloor cn + d \rfloor - n\lfloor cm + d \rfloor - (m-n)I_1| < \frac{2}{|nm|}|m(cn+d) - n(cm+d) + m + n - (m-n)I_1| = \frac{2}{|nm|}|(n-m)(I_1 - d) + m + n| < 2|\frac{(n+m)(I_1-d)+m+n}{nm}| = 2|\frac{(m+n)(I_1-d+1)}{nm}| = 2|I_1 - d + 1|\frac{m+n}{nm} = 2|I_1 - d + 1|\left(\frac{1}{n} + \frac{1}{m}\right) < 2|I_1 - d + 1|\frac{2}{N} = \frac{4|I_1-d+1|}{N} < \epsilon$. by knowing that $\lfloor cn + d \rfloor > \lfloor cm + d \rfloor$, $R(i) < 2$ for any i and Lemma S12. □

To prove the existence of the limit in Lemma S13, note that $\lceil x \rceil = x + frac(-x)$, for any real number x (heed that using this definition of $frac$, $frac(1.7) = 0.7$ and $frac(-1.7) = 0.3$), because $frac(-x) = -x - \lfloor -x \rfloor = -x - (-\lceil x \rceil) = -x + \lceil x \rceil \Leftrightarrow \lceil x \rceil = x + frac(-x)$ by the definition of $\lfloor -x \rfloor$ and $\lfloor -x \rfloor = -\lceil x \rceil$. Thus, $\lim_{T\to\infty} \frac{1}{T} \sum_{x_h=n_l^-+1}^{\min(n_l^+-1,K'-1)} \left(\lfloor Y_2^R(x_h) \rfloor - \lceil Y_1^R(x_h) \rceil + 1 \right) = \lim_{T\to\infty} \frac{1}{T} \sum_{x_h=n_l^-+1}^{\min(n_l^+-1,K'-1)} \left(Y_2^R(x_h) - Y_1^R(x_h) + 1 \right) - \lim_{T\to\infty} \frac{1}{T} \sum_{x_h=n_l^-+1}^{\min(n_l^+-1,K'-1)} \left(frac\left(- Y_1^R(x_h)\right) + frac\left(Y_2^R(x_h)\right)\right)$. The limit of the first term above exists and its value is presented below on (S42). The existence of the limit for the second term was shown by Lemma S13 for any outcome of $\min(n_l^+ - 1, K' - 1)$, because, if $\left\lfloor \frac{2(vT-s)\cos(\pi/6-\theta)+2s\sin(|\pi/6-\theta|)}{\sqrt{3}d} \right\rfloor = n_l^+ - 1 \leq K' - 1$, then $c = \frac{2v\cos(\psi-\pi/6)}{\sqrt{3}d}$ and $d = \frac{2s}{\sqrt{3}d}(\sin(|\pi/6 - \theta|) - \cos(\pi/6 - \theta))$ on the Lemma S13. If $n_l^+ - 1 > K' - 1 = \left\lceil \frac{2}{\sqrt{3}d}((vT - s)\cos(\psi - \pi/6) - 2s\sin(|\psi - \pi/6|)) - 1 \right\rceil$, as for any x, $\lceil x \rceil = \lfloor x \rfloor$ or $\lceil x \rceil = \lfloor x \rfloor + 1$ depending on whether x is an integer or not, then $K' - 1 = \left\lfloor \frac{2(vT-s)\cos(\psi-\pi/6)}{\sqrt{3}d} - \frac{2s\sin(|\psi-\pi/6|)}{\sqrt{3}d} - 1 \right\rfloor$ or $K' - 1 = \left\lfloor \frac{2(vT-s)\cos(\psi-\pi/6)}{\sqrt{3}d} - \frac{2s\sin(|\psi-\pi/6|)}{\sqrt{3}d} \right\rfloor$. For both cases, on the Lemma S13 $c = \frac{2v\cos(\psi-\pi/6)}{\sqrt{3}d}$ as well, but for the former case, $d = -\frac{2s(\sin(|\psi-\pi/6|)+\cos(\pi/6-\theta))}{\sqrt{3}d} - 1$, and for the latter, $d = -\frac{2s(\sin(|\psi-\pi/6|)+\cos(\pi/6-\theta))}{\sqrt{3}d}$.

To get the bounds,

$$\begin{aligned}
&\lim_{T\to\infty}\frac{1}{T}\sum_{x_h=n_l^-+1}^{\min(n_l^+-1,K'-1)}\left(Y_2^R(x_h)-Y_1^R(x_h)-1\right)\\
&<\lim_{T\to\infty}\frac{1}{T}\sum_{x_h=n_l^-+1}^{\min(n_l^+-1,K'-1)}\left(\lfloor Y_2^R(x_h)\rfloor-\lceil Y_1^R(x_h)\rceil+1\right)\\
&\leq\lim_{T\to\infty}\frac{1}{T}\sum_{x_h=n_l^-+1}^{\min(n_l^+-1,K'-1)}\left(Y_2^R(x_h)-Y_1^R(x_h)+1\right),
\end{aligned}\tag{S40}$$

and by Lemma S6, as $T\to\infty$, $Y_2^R(x_h)-Y_1^R(x_h)=\frac{\frac{y_2}{d}+\tan(\psi)x_h}{\frac{\sqrt{3}+\tan(\psi)}{2}}-\frac{\frac{y_1}{d}+\tan(\psi)x_h}{\frac{\sqrt{3}+\tan(\psi)}{2}}=\frac{2s}{d\cos(\psi-\pi/6)}$, by (S4).

For the first limit at (S40) in the case of $\min(n_l^+-1,K'-1)=n_l^+-1$,

$$\lim_{T\to\infty}\frac{1}{T}\sum_{x_h=n_l^-+1}^{n_l^+-1}\left(Y_2^R(x_h)-Y_1^R(x_h)-1\right)=\frac{4vs}{\sqrt{3}d^2}-\frac{2v\cos(\psi-\pi/6)}{\sqrt{3}d}.\tag{S41}$$

Above $\lim_{T\to\infty}\frac{1}{T}n_l^+=\frac{2v\cos(\psi-\pi/6)}{\sqrt{3}d}$ is derived by using the sandwich theorem and the inequality $x-1<\lfloor x\rfloor\leq x$ to get the bounds on n_l^+.

Similarly, for the last limit at (S40) in the case of $\min(n_l^+-1,K'-1)=n_l^+-1$, $\lim_{T\to\infty}\frac{1}{T}\sum_{x_h=n_l^-+1}^{n_l^+-1}(Y_2^R(x_h)-Y_1^R(x_h)+1)=\frac{4vs}{\sqrt{3}d^2}+\frac{2v\cos(\psi-\pi/6)}{\sqrt{3}d}$. The limits above in the case of $\min(n_l^+-1,K'-1)=K'-1$ yields the same result because of the sandwich theorem, the inequality $x\leq\lceil x\rceil<x+1$, and $\frac{2v\cos(\psi-\pi/6)}{\sqrt{3}d}=\lim_{T\to\infty}\frac{1}{T}\left((2(vT-s)\cos(\psi-\pi/6)-2s\sin(|\psi-\pi/6|))/(\sqrt{3}d)\right)\leq\lim_{T\to\infty}\frac{1}{T}(K'-1)=\lim_{T\to\infty}\frac{1}{T}K'=\lim_{T\to\infty}\frac{1}{T}\left\lceil(2(vT-s)\cos(\psi-\pi/6)-2s\sin(|\psi-\pi/6|))/(\sqrt{3}d)\right\rceil<\lim_{T\to\infty}\frac{1}{T}\left(\frac{2(vT-s)\cos(\psi-\pi/6)-2s\sin(|\psi-\pi/6|)}{\sqrt{3}d}+1\right)=\frac{2v\cos(\psi-\pi/6)}{\sqrt{3}d}$, so, $\lim_{T\to\infty}\frac{1}{T}K'=\lim_{T\to\infty}\frac{1}{T}n_l^+$. Consequently, the limit below exists and

$$\lim_{T\to\infty}\frac{1}{T}\sum_{x_h=n_l^-+1}^{\min(n_l^+-1,K'-1)}\left(Y_2^R(x_h)-Y_1^R(x_h)+1\right)=\frac{4vs}{\sqrt{3}d^2}+\frac{2v\cos(\psi-\frac{\pi}{6})}{\sqrt{3}d}.\tag{S42}$$

Finally, using the bounds provided by (S41) and (S42) the expected result is obtained. □

By Lemmas S9, S10 and S11 it is obtained for $\psi\neq\pi/6$

$$\lim_{T\to\infty}f_h(T,\psi)\in\left(\frac{4vs}{\sqrt{3}d^2}-\frac{2v\cos(\psi-\pi/6)}{\sqrt{3}d},\frac{4vs}{\sqrt{3}d^2}+\frac{2v\cos(\psi-\pi/6)}{\sqrt{3}d}\right].\tag{S43}$$

For $\psi=\pi/6$, by (S18), $\lim_{T\to\infty}\frac{1}{T}\sum_{x_h=0}^{\left\lfloor\frac{2(vT-s)}{\sqrt{3}d}\right\rfloor}\left(\frac{\sqrt{3}y_2+dx_h}{2d}-\frac{\sqrt{3}y_1+dx_h}{2d}-1\right)<\lim_{T\to\infty}f_h(T,\pi/6)\leq\lim_{T\to\infty}\frac{1}{T}\sum_{x_h=0}^{\left\lfloor\frac{2(vT-s)}{\sqrt{3}d}\right\rfloor}\left(\frac{\sqrt{3}y_2+dx_h}{2d}-\frac{\sqrt{3}y_1+dx_h}{2d}+1\right)$, with $\lim_{T\to\infty}\frac{1}{T}\sum_{x_h=0}^{\left\lfloor\frac{2(vT-s)}{\sqrt{3}d}\right\rfloor}\left(\frac{\sqrt{3}y_2+dx_h}{2d}-\frac{\sqrt{3}y_1+dx_h}{2d}+1\right)=\lim_{T\to\infty}\frac{1}{T}\sum_{x_h=0}^{\left\lfloor\frac{2(vT-s)}{\sqrt{3}d}\right\rfloor}\left(\frac{\sqrt{3}s}{d\cos(\pi/6)}+1\right)=\lim_{T\to\infty}\frac{1}{T}\left\lfloor\frac{2(vT-s)}{\sqrt{3}d}+1\right\rfloor\left(\frac{2s}{d}+1\right)=\frac{2v}{\sqrt{3}d}\left(\frac{2s}{d}+1\right)$, from (S4) and, as similarly done before, $\lim_{T\to\infty}\frac{1}{T}\left\lfloor\frac{2(vT-s)}{\sqrt{3}d}+1\right\rfloor=\frac{2v}{\sqrt{3}d}$ by using the sandwich theorem and the inequality $x-1<\lfloor x\rfloor\leq x$ to get the bounds on the

floor function; and $\lim_{T\to\infty} \frac{1}{T} \sum_{x_h=0}^{\left\lfloor \frac{2(vT-s)}{\sqrt{3}d} \right\rfloor} \left(\frac{\sqrt{3}y_2+dx_h}{2d} - \frac{\sqrt{3}y_1+dx_h}{2d} - 1 \right) = \frac{2v}{\sqrt{3}d}\left(\frac{2s}{d} - 1\right)$. Accordingly, $\lim_{T\to\infty} f_h(T, \pi/6) \in \left(\frac{2v}{\sqrt{3}d}\left(\frac{2s}{d} - 1\right), \frac{2v}{\sqrt{3}d}\left(\frac{2s}{d} + 1\right)\right]$, which are the same values in (S43) if $\psi = \pi/6$ is used. Lemmas S1–S6, S9, S10 and S11 used ψ, so, after replacing ψ by $\pi/3 - \theta$, the proof of the Proposition 6 is concluded.

Proof of Lemma 2

Figure 12b shows the distance d_r from the target centre where the robots begin turning. By symmetry, this is the same distance from the target centre where the robots stop turning. From the right triangle ABC on that figure, $|\overline{AC}| = \sqrt{(r+s)^2 - (r+d/2)^2}$ and from $\triangle ACD$, $d_r = \sqrt{(d/2)^2 + |\overline{AC}|^2}$. Thus, $d_r = \sqrt{(d/2)^2 + (r+s)^2 - (r+d/2)^2} = \sqrt{s(2r+s) - rd}$.

Proof of Lemma 3

From Figure 12b, it can be seen that the right triangle ABE has angle $\widehat{EAB} = \alpha/2$, hypotenuse $r+s$ and cathetus $r+d/2$. Hence, it directly follows that $sin(\alpha/2) = \frac{r+d/2}{r+s} \Leftrightarrow r = \frac{s\sin(\alpha/2) - d/2}{1-\sin(\alpha/2)}$.

Proof of Proposition 7

The number of trajectories K must be greater or equal to 3. The reason is that for the minimum possible value for s, $s = d/2$, $K = 2$ is enough to have parallel lanes. However, starting with $K = 3$, curved trajectories are needed to guarantee that robots of one lane do not interfere with robots from another lane.

Also, there are K identical trajectories around the target, each taking a central angle of α. As a result, the value of α given K is $\alpha = \frac{2\pi}{K}$, implying that $0 < \alpha \leq \frac{2\pi}{3}$.

Additionally, in the worst case, one robot in each lane arrives in the target region at the same time. When robots of all lanes simultaneously occupy the target region, their positions can be seen as the vertices of a regular polygon which must be inscribed in the circular target region of radius s (e.g., Figure 13 has a square whose sides are greater than d). The number of robots on the target region at the same time must be limited by the maximum number of sides of an inscribed regular polygon with a minimum side greater than or equal to d. The side of a K regular polygon inscribed in a circle of radius s measures $2s\sin\left(\frac{\pi}{K}\right)$. Thence, $2s\sin\left(\frac{\pi}{K}\right) \geq d \Rightarrow \frac{\pi}{\arcsin\left(\frac{d}{2s}\right)} \geq K$.

Proof of Proposition 8

Using the touch and run strategy, each lane is distant by at least d from each other. However, the minimum distance between robots on the same lane d_o must be checked at the beginning of the curved path, as their distance decreases if assuming constant linear speed. Two cases are distinguished based on Figure S14:

1. $|\overline{ED}| < d$: Two robots cannot be on the lane curved path;
2. $|\overline{ED}| \geq d$: More than one robot can occupy the lane curved path.

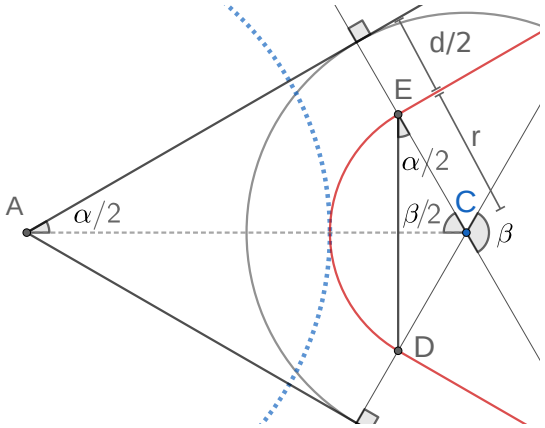

Figure S14. Relationship between the curved path and the distance between the robots.

In this figure, the red line represents the trajectory of robots in one lane. α is the central angle for the lane. The dashed blue circle of centre A is the target. C is the centre of the circle of radius r from the circular trajectory. The grey circle of centre C has a radius of $r + d/2$. Points D and E represent the connection between the curved path and the straight path. $\beta = \pi - \alpha$ due to the symmetry and the fact that the sum of the angles of $\triangle ECD$ is equal to π.

The two identified cases affect the minimum distance between robots, d_o, such that they can follow the trajectory without decreasing their linear speed. In both cases, they need to satisfy the minimum distance d if they are turning on the curved path. From Figure S14,

$$|\overline{ED}| = 2r\sin\left(\frac{\beta}{2}\right) = 2r\sin\left(\frac{\pi}{2} - \frac{\alpha}{2}\right) = 2r\cos\left(\frac{\alpha}{2}\right). \tag{S44}$$

In case 1, in Figure S15a, two points T and U are defined on the lane such that the distance between them is $|\overline{TU}| = d$ and their distances to the target are equal. The robots R_1 and R_2 are the black dots on the red line representing the trajectory. If the delay between R_1 and R_2 is less than the time for a robot to run from T to U following the red trajectory, there will be some instant in which R_1 and R_2 will be vertically aligned. Their positions at that instant are represented by grey dots in front of them. Hence, their distance would be less than d. The right triangle TVE has side $\overline{TV}$, which can be measured using $\overline{ED}$. The delay between one robot at T and another at U is equal to $\Delta t_1 = \frac{1}{v}\left(|\overline{TE}| + |\widehat{ED}| + |\overline{DU}|\right)$, that is, the time for running through the straight line TE, the curved path ED and the straight line DU.

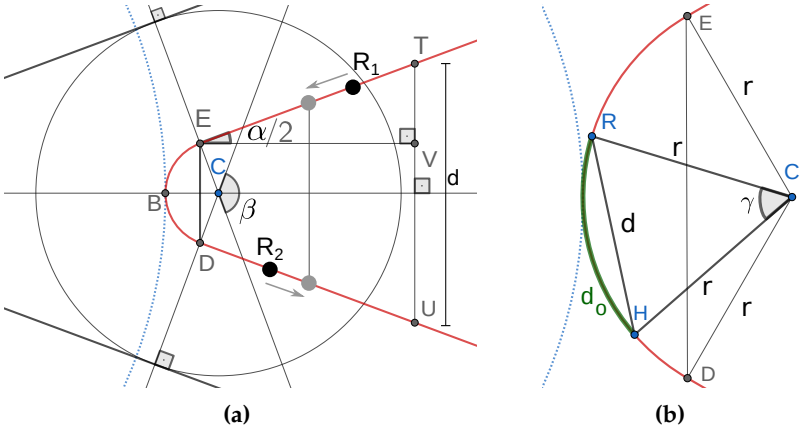

Figure S15. Enlargements of Figure S14. **(a)** $|\overline{ED}| < d$. **(b)** $|\overline{ED}| \geq d$

For any delay less than Δt_1 between two robots, say R_1 and R_2, there is an instant of time when R_1 is on the path between B and T and R_2 is on the path between B and U, and they are vertically aligned (Figure S15a). In this case, the distance between R_1 and R_2 is below $|\overline{TU}|$, so they do not respect the minimum distance d between them. Hence, the minimum delay between two robots in case 1 is Δt_1.

From Figure S14, $|\widehat{ED}| = r\beta = r(\pi - \alpha)$. For calculating the value of $|\overline{TE}|$ and $|\overline{DU}|$ from Figure S15a, observe that $|\overline{TE}| = |\overline{DU}|$ by symmetry. Thus, $|\overline{VT}| = \frac{d}{2} - \frac{|\overline{ED}|}{2} = \frac{d}{2} - r\cos\left(\frac{\alpha}{2}\right)$ From Figure S15a and (S44). As $\triangle TVE$ is right, $|\overline{TE}| = \frac{|\overline{VT}|}{\sin(\alpha/2)}$. Thence, $\Delta t_1 = \frac{1}{v}\left(r(\pi-\alpha) + 2\frac{d/2 - r\cos(\alpha/2)}{\sin(\alpha/2)}\right) = \frac{r(\pi-\alpha)}{v} + \frac{d-2r\cos(\alpha/2)}{v\sin(\alpha/2)}$ and $d_o = \max(d, v\Delta t_1) = \max\left(d, r(\pi-\alpha) + \frac{d-2r\cos(\alpha/2)}{\sin(\alpha/2)}\right)$. Here the max function is used because the result of $v\Delta t_1$ can still be less than d, depending on α, r and d.

In case 2, one has to check the minimum distance d when two robots are on the circular part $\widehat{ED}$ in Figure S15b. Here, d_o denotes the minimum arc length for two robots located at any two points R and H on $\widehat{ED}$ such that they are distant by at least d. γ is the angle defining the arc d_o for the circle of centre C. From this figure, $\triangle CRH$ is isosceles, so $\gamma = 2\arcsin\left(\frac{d}{2r}\right)$. Thus, to keep constant linear speed, the delay between two robots in this case is $\Delta t_2 = \frac{d_o}{v} = \frac{r\gamma}{v} = \frac{2r}{v}\arcsin\left(\frac{d}{2r}\right)$. Then, $d_o = \max(d, v\Delta t_2) = \max\left(d, 2r\arcsin\left(\frac{d}{2r}\right)\right)$. The max function is applied for a similar reason as exposed before. After rearranging, (17) and (18) are obtained.

For calculating the throughput $f_t(K,T)$ for K lanes and a given time T after the arrival of the first robot, the number of robots reaching the target region by the time T is obtained, then the Definition 2 is applied. As it was assumed that the first robot of every lane begins at the same distance from the target, at time $T = 0$ there are K robots simultaneously arriving. Then, after d_o/v units of time, there are K more robots arriving and this keeps happening every d_o/v units of time. Denote $N(K,T)$ the total number of robots that have arrived at the target region from K lanes by time T. Thus, $N(K,T) = K\left\lfloor \frac{T}{\frac{d_0}{v}} + 1 \right\rfloor = K\left\lfloor \frac{vT}{d_o} + 1 \right\rfloor$, so, by Definition 2, $f_t(K,T) = \frac{1}{T}\left(K\left\lfloor \frac{vT}{d_o} + 1 \right\rfloor - 1\right)$.

As for every number x, $\lfloor x \rfloor = x - frac(x)$ and $0 \leq frac(x) < 1$, then distributing $\frac{1}{T}$ for each term, $f_t(K) = \lim_{T\to\infty} f_t(K,T) = \frac{Kv}{d_o}$.

Proof of Proposition 9

For any $u < \frac{\sqrt{3}+2}{4-2\sqrt{3}}$, $(2u+1)\frac{v}{d} > f_h^{min}(u)$, due to

$$(2u+1)\frac{v}{d} > \frac{2}{\sqrt{3}}(2u-1)\frac{v}{d} \Leftrightarrow u < \frac{-1-\frac{2}{\sqrt{3}}}{2-\frac{4}{\sqrt{3}}} = \frac{\sqrt{3}+2}{4-2\sqrt{3}}. \tag{S45}$$

$f_p(u) = (2u+1)\frac{v}{d}$ when $2u+1 \in \mathbb{Z}$. Also, as $u < \frac{\sqrt{3}+2}{4-2\sqrt{3}} < 7$, u can be a number satisfying $(2u+1) = \lfloor 2u+1 \rfloor$. Thus, there are some values of u such that $f_p(u) = \lfloor 2u+1 \rfloor \frac{v}{d} > f_h^{min}(u)$.

From the equivalence in (S45) and because for any x, $\lfloor x \rfloor \leq x$, it follows that for any $u \geq \frac{\sqrt{3}+2}{4-2\sqrt{3}}$, $f_p(u) \leq (2u+1)\frac{v}{d} \leq f_h^{min}(u)$.

References

1. Chang, H.C.; Wang, L.C. A Simple Proof of Thue's Theorem on Circle Packing. *arXiv* **2010**, arXiv:math.MG/1009.4322.
2. Red Blob Games. Hexagonal Grids. 2021. Available online: https://www.redblobgames.com/grids/hexagons/ (accessed on 16 November 2021).
3. Graham, R.L.; Knuth, D.E.; Patashnik, O. *Concrete Mathematics: A Foundation for Computer Science*, 2nd ed.; Addison-Wesley Professional: Reading, MA, USA, 1994.